

**Supporting Information for**

**Helically chiral Pd(II) complexes containing intramolecular Pd···Pd metallophilicity as circularly polarized molecular phosphors**

Jinqiang Lin, Mo Xie, Xiaobao Zhang, Qin Gao, Xiaoyong Chang, Chao Zou\*, and Wei Lu\*

*Department of Chemistry, South University of Science and Technology of China  
Shenzhen, Guangdong 518055, P. R. China*

*E-mail:* [zouc@sustech.edu.cn](mailto:zouc@sustech.edu.cn), [luw@sustech.edu.cn](mailto:luw@sustech.edu.cn)

## Experimental Section

**Materials.** All reagents were purchased from commercial sources and used as received. The solvents used for synthesis were of analytical grade unless stated otherwise. The chiral ligands 7,7-dimethyl-3-(6-phenylpyridin-2-yl)-5,6,7,8-tetrahydro-6,8-methanoisoquinoline (**HC<sup>N</sup>N<sup>\*</sup>(S)**) and **HC<sup>N</sup>N<sup>\*</sup>(R)**),<sup>1</sup> 1,2-bis(2-ethynylphenyl)ethyne,<sup>2</sup> and 1,2-bis(2,6-diethynylphenyl)ethyne<sup>3</sup> were prepared according to literature methods.

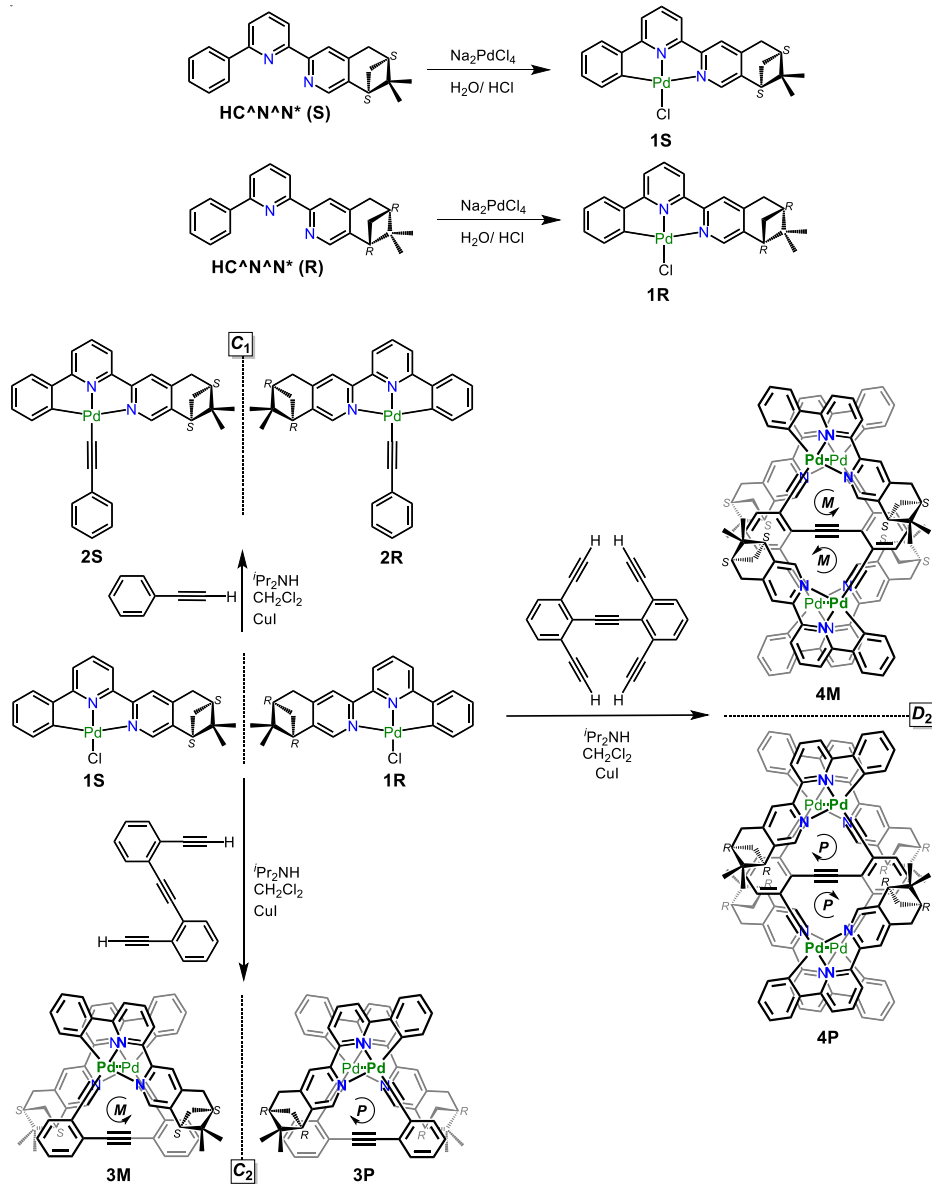
**Characterization.** <sup>1</sup>H, <sup>13</sup>C, <sup>19</sup>F, NMR spectra were recorded with Bruker Avance 400 FT-NMR or 500 FT-NMR spectrometers. Infrared spectra were recorded on a Bruker V80 spectrometer. UV-Vis absorption spectra were recorded on a Thermo Scientific Evolution 201 UV-Visible Spectrophotometer. HR-MS (high resolution mass spectra) were obtained on a Thermo Scientific Q Exactive mass spectrometer, operated in heated electrospray ionization (HESI) mode, coupled with Thermo Scientific Ultimate 3000 system. Photo-luminescent properties (solution and solid) were recorded via Edinburg spectrometer FLS-980 equipped with MCP-PMT and NIR-PMT detectors. Emission lifetime measurements were performed with Hamamatsu compact fluorescence lifetime spectrometer C11367. Absolute luminescent quantum yields were recorded with Hamamatsu absolute PL quantum yield spectrometer C11347. Circular dichroism (CD) spectra were recorded with Applied Photophysics Chirascan circular dichroism spectrometers. Circularly polarized luminescence (CPL) spectra were performed on a JASCO CPL-200 spectrometer at National Center for Nanoscience and Technology, China and a JASCO CPL-300 spectrometer at SUSTech, China. The solvent CH<sub>2</sub>Cl<sub>2</sub> used for spectroscopic measurements was freshly distilled over CaH<sub>2</sub>.

Single crystals of **3P** and **3M** suitable for X-ray diffraction analysis were obtained by diffusion of Et<sub>2</sub>O into their CHCl<sub>3</sub> solution. The diffraction data were collected by

- 
- (1) P. G. Bomben, K. C. D. Robson, P. A. Sedach, C. P. Berlinguette. *Inorg. Chem.* **2009**, *48*, 9631.
  - (2) J. Lin, C. Zou, X. Zhang, Q. Gao, S. Suo, Q. Zhuo, X. Chang, M. Xie, W. Lu, *Dalton Trans.*, **2019**, *48*, 10417.
  - (3) J. D. Bradshaw, L. Guo, C. A. Tessier, W. J. Youngs, *Organometallics*. **1996**, *15*, 2582.

a 'Bruker APEX-II CCD' diffractometer. The crystal was kept at 100 K during data collection. Using Olex2, the structure was solved with the XT structure solution program using Direct Methods and refined with the XL refinement package using Least Squares minimization.

### Synthesis and characterization.



**Synthesis of **1R**.** To a suspension of  $\text{Na}_2\text{PdCl}_4$  (882 mg, 3 mmol) and **HC<sup>N</sup>N<sup>\*</sup>(R)** (980 mg, 3 mmol) in 40 mL water was added concentrated hydrochloric acid (3 mL).

The mixture was heated to 95 °C and stirred overnight. Yellow solid product was obtained by filtration and washed with H<sub>2</sub>O, MeOH and Et<sub>2</sub>O successively. Yield: 90%. <sup>1</sup>H NMR (400 MHz, DMSO) δ 8.38 (s, 1H), 8.27–8.10 (m, 3H), 8.00 (dd, *J* = 7.0, 2.0 Hz, 1H), 7.65 (dd, *J* = 7.2, 1.9 Hz, 1H), 7.53 (dd, *J* = 7.1, 1.8 Hz, 1H), 7.19–7.01 (m, 2H), 3.25–3.06 (m, 2H), 3.03 (t, *J* = 5.4 Hz, 1H), 2.81–2.69 (m, 1H), 2.40–2.26 (m, 1H), 1.42 (s, 3H), 1.20 (d, *J* = 9.8 Hz, 1H), 0.65 (s, 3H). HR-MS (ESI): m/z = 472.1003, [M–Cl+CH<sub>3</sub>CN]<sup>+</sup>, calc. for [C<sub>23</sub>H<sub>21</sub>ClN<sub>2</sub>Pd–Cl+CH<sub>3</sub>CN]<sup>+</sup> m/z = 472.1005.

**Synthesis of 1S.** The complex was prepared by the same method as that used for **1R** except that **HC<sup>N</sup>N<sup>\*</sup>(S)** was used as the precursor. Yield: 88%. <sup>1</sup>H NMR (500 MHz, DMSO) δ 8.37 (s, 1H), 8.29–8.11 (m, 3H), 8.00 (d, *J* = 6.9 Hz, 1H), 7.65 (d, *J* = 7.6 Hz, 1H), 7.53 (d, *J* = 6.8 Hz, 1H), 7.09 (dt, *J* = 14.5, 7.1 Hz, 2H), 3.22–3.07 (m, 2H), 3.02 (t, *J* = 5.0 Hz, 1H), 2.81–2.71 (m, 1H), 2.40–2.25 (m, 2H), 1.42 (s, 3H), 1.20 (d, *J* = 9.8 Hz, 1H), 0.65 (s, 3H). HR-MS (ESI): m/z = 472.1005, [M–Cl+CH<sub>3</sub>CN]<sup>+</sup>, calc. for [C<sub>23</sub>H<sub>21</sub>ClN<sub>2</sub>Pd–Cl+CH<sub>3</sub>CN]<sup>+</sup> m/z = 472.1005.

**Synthesis of 2R.** To a suspension of **1R** (47 mg, 0.1 mmol) and CuI (ca. 1 mg) in 8 mL dichloromethane under N<sub>2</sub> was added ethynylbenzene (24 mg, 0.24 mmol) and diisopropylamine (2.5 mL). The mixture was stirred at room temperature overnight, and then the solvent was evaporated to dryness. The residue was washed thoroughly with MeOH and Et<sub>2</sub>O, and recrystallized from CHCl<sub>3</sub> and Et<sub>2</sub>O to give the pure product. Yield: 55%. <sup>1</sup>H NMR (500 MHz, DMSO) δ 8.38 (s, 1H), 8.35 (s, 1H), 8.23–8.10 (m, 2H), 8.00 (d, *J* = 7.9 Hz, 1H), 7.87–7.79 (m, 1H), 7.69 (dd, *J* = 7.1, 2.0 Hz, 1H), 7.42–7.33 (m, 2H), 7.27 (t, *J* = 7.7 Hz, 2H), 7.16 (t, *J* = 7.4 Hz, 1H), 7.15–7.06 (m, 2H), 3.15 (dd, *J* = 37.1, 16.2 Hz, 3H), 3.05 (t, *J* = 5.4 Hz, 1H), 2.80–2.71 (m, 1H), 2.35 (t, *J* = 5.6 Hz, 2H), 2.08–1.91 (m, 2H), 1.42 (s, 3H), 0.67 (s, 3H). HR-MS (ESI): m/z = 555.1023, [M+Na]<sup>+</sup>, calc. for [C<sub>31</sub>H<sub>26</sub>N<sub>2</sub>Pd+Na]<sup>+</sup> m/z = 555.1044. IR: 2095 cm<sup>-1</sup> ν(C≡C).

**Synthesis of 2S.** The complex was prepared using the same procedure as that used for **2R** except that **1S** was used as the precursor. Yield: 49%. <sup>1</sup>H NMR (400 MHz, CDCl<sub>3</sub>) δ 8.57 (s, 1H), 8.08 (d, *J* = 7.5 Hz, 1H), 7.82 (t, *J* = 8.0 Hz, 1H), 7.69 (s, 1H), 7.57 (dd,

$J = 11.0, 4.6$  Hz, 3H), 7.44 (d,  $J = 7.6$  Hz, 1H), 7.28–7.24 (m, 3H), 7.20–7.12 (m, 2H), 7.07 (dd,  $J = 7.4, 6.3$  Hz, 1H), 3.10 (s, 2H), 2.98 (t,  $J = 5.5$  Hz, 2H), 2.85–2.67 (m, 2H), 2.50–2.30 (m, 2H), 2.01 (dd,  $J = 12.1, 6.0$  Hz, 2H), 1.44 (s, 3H), 0.68 (s, 3H).  $^{13}\text{C}$  NMR (126 MHz,  $\text{CDCl}_3$ )  $\delta$  163.72, 155.66, 154.31, 153.75, 148.31, 148.21, 140.50, 138.69, 131.64, 130.60, 128.49, 127.85, 125.06, 124.14, 123.97, 121.21, 118.03, 117.03, 44.51, 39.68, 39.16, 33.32, 31.29, 25.75, 21.44. HR-MS (ESI): m/z = 555.1026,  $[\text{M}+\text{Na}]^+$ , calc. for  $[\text{C}_{31}\text{H}_{26}\text{N}_2\text{Pd}+\text{Na}]^+$  m/z = 555.1044. IR: 2095  $\text{cm}^{-1}$  v(C≡C).

**Synthesis of 3P.** To a suspension of **1R** (94 mg, 0.2 mmol) and CuI (ca. 1 mg) in 12 mL dichloromethane under  $\text{N}_2$  was added 1,2-bis(2-ethynylphenyl)ethyne (23 mg, 0.1 mmol) and diisopropylamine (3 mL). The mixture was stirred at room temperature overnight, and then the solvent was evaporated to dryness. The residue was washed thoroughly with MeOH and  $\text{Et}_2\text{O}$ , and recrystallized from  $\text{CHCl}_3$  and  $\text{Et}_2\text{O}$  to give the pure product. Yield: 65%.  $^1\text{H}$  NMR (400 MHz, DMSO)  $\delta$  8.88 (s, 2H), 7.71 (t,  $J = 8.0$  Hz, 2H), 7.64–7.48 (m, 4H), 7.41 (d,  $J = 8.0$  Hz, 2H), 7.37 (d,  $J = 8.0$  Hz, 2H), 7.34–7.09 (m, 8H), 7.06 (d,  $J = 7.2$  Hz, 2H), 6.87 (t,  $J = 7.4$  Hz, 2H), 6.74 (t,  $J = 7.1$  Hz, 2H), 2.99 (dd,  $J = 31.1, 17.1$  Hz, 4H), 2.30–2.13 (m, 4H), 2.12–1.94 (m, 4H), 1.10 (s, 6H), 0.54 (s, 6H).  $^1\text{H}$  NMR (500 MHz,  $\text{CD}_2\text{Cl}_2$ )  $\delta$  9.03 (s, 1H), 7.61 (dd,  $J = 7.5, 1.5$  Hz, 1H), 7.50 (t,  $J = 7.9$  Hz, 1H), 7.35 (dd,  $J = 7.5, 1.3$  Hz, 1H), 7.23–7.11 (m, 1H), 7.10–7.05 (m, 1H), 6.97 (d,  $J = 7.6$  Hz, 1H), 6.93 (d,  $J = 7.9$  Hz, 1H), 6.87 (td,  $J = 7.4, 1.1$  Hz, 1H), 6.76 (td,  $J = 7.3, 1.1$  Hz, 1H), 3.02–2.88 (m, 1H), 2.29–2.21 (m, 1H), 2.21–2.15 (m, 1H), 2.12 (t,  $J = 5.3$  Hz, 1H), 1.16 (dd,  $J = 12.3, 5.4$  Hz, 1H), 1.12 (s, 1H), 0.54 (s, 1H).  $^{13}\text{C}$  NMR (126 MHz,  $\text{CD}_2\text{Cl}_2$ )  $\delta$  162.33, 158.59, 154.83, 154.13, 151.59, 148.58, 146.67, 139.54, 137.90, 132.91, 132.84, 131.19, 129.20, 127.80, 127.54, 125.68, 124.54, 123.61, 123.27, 121.06, 117.32, 117.27, 102.39, 93.25, 45.12, 40.03, 38.73, 33.72, 33.05, 25.67, 21.31. HR-MS (ESI): m/z = 1089.2197,  $[\text{M}+\text{H}]^+$ , calc. for  $[\text{C}_{64}\text{H}_{50}\text{N}_4\text{Pd}_2+\text{H}]^+$  m/z = 1089.2182. IR: 2096  $\text{cm}^{-1}$  v(C≡C).

**Synthesis of 3M.** The complex was prepared using the same procedure as that used for **3P** except that **1S** was used as the precursor. Yield: 71%.  $^1\text{H}$  NMR (500 MHz, DMSO)

$\delta$  8.87 (s, 2H), 7.71 (t,  $J$  = 7.9 Hz, 2H), 7.63–7.50 (m, 4H), 7.41 (d,  $J$  = 8.0 Hz, 2H), 7.37 (d,  $J$  = 8.0 Hz, 2H), 7.32–7.11 (m, 8H), 7.06 (d,  $J$  = 7.4 Hz, 2H), 6.87 (t,  $J$  = 7.4 Hz, 2H), 6.74 (t,  $J$  = 7.2 Hz, 2H), 2.99 (dd,  $J$  = 36.8, 16.8 Hz, 5H), 2.33–2.23 (m, 1H), 2.23–2.15 (m, 1H), 2.08–1.93 (m, 4H), 1.10 (s, 6H), 0.54 (s, 6H). HR-MS (ESI): m/z = 1089.2185, [M+H]<sup>+</sup>, calc. for [C<sub>64</sub>H<sub>50</sub>N<sub>4</sub>Pd<sub>2</sub>+H]<sup>+</sup> m/z = 1089.2182. IR: 2096 cm<sup>-1</sup> v(C≡C).

**Synthesis of 4P.** To a suspension of **1R** (47 mg, 0.1 mmol) and CuI (ca. 1 mg) in 12 mL dichloromethane under N<sub>2</sub> was added 1,2-bis(2,6-diethynylphenyl)ethyne (13 mg, 0.05 mmol) and diisopropylamine (3 mL). The mixture was stirred at room temperature overnight, and then the solvent was evaporated to dryness. The residue was washed thoroughly with MeOH and Et<sub>2</sub>O, and recrystallized from CHCl<sub>3</sub> and Et<sub>2</sub>O to give the pure product. Yield: 7%. <sup>1</sup>H NMR (500 MHz, DMSO)  $\delta$  8.78 (s, 4H), 7.72 (t,  $J$  = 7.8 Hz, 4H), 7.42 (s, 4H), 7.36 (dd,  $J$  = 12.8, 8.1 Hz, 8H), 7.24–7.19 (m, 2H), 7.16 (dt,  $J$  = 51.1, 8.2 Hz, 12H), 6.86 (t,  $J$  = 7.1 Hz, 4H), 6.68 (t,  $J$  = 6.9 Hz, 4H), 2.98 (dd,  $J$  = 56.5, 17.0 Hz, 8H), 2.24 (s, 6H), 2.08–1.91 (m, 4H), 1.76 (s, 4H), 1.33 (d,  $J$  = 9.7 Hz, 4H), 1.16 (s, 12H), 0.52 (s, 12H). HR-MS (ESI): m/z = 1997.3593, [M+H]<sup>+</sup>, calc. for [C<sub>114</sub>H<sub>90</sub>N<sub>8</sub>Pd<sub>4</sub>+H]<sup>+</sup> m/z = 1997.3554. IR: 2089 cm<sup>-1</sup> v(C≡C).

**Synthesis of 4M.** The complex was prepared using the same procedure as that used for **4P** except that **1S** was used as the precursor. Yield: 5%. <sup>1</sup>H NMR (500 MHz, CDCl<sub>3</sub>)  $\delta$  9.08 (s, 4H), 7.49 (t,  $J$  = 7.9 Hz, 4H), 7.41 (d,  $J$  = 7.1 Hz, 4H), 7.35 (d,  $J$  = 7.6 Hz, 4H), 7.08–7.05 (m, 2H), 7.01 (d,  $J$  = 8.0 Hz, 4H), 6.97 (d,  $J$  = 7.9 Hz, 8H), 6.93 (s, 4H), 6.85 (t,  $J$  = 7.4 Hz, 4H), 6.73 (t,  $J$  = 7.0 Hz, 4H), 2.94 (d,  $J$  = 27.0 Hz, 8H), 2.58–2.54 (m, 4H), 2.26–2.17 (m, 8H), 2.05–2.01 (m, 4H), 1.16 (s, 12H), 0.50 (s, 12H). HR-MS (ESI): m/z = 1997.3580, [M+H]<sup>+</sup>, calc. for [C<sub>114</sub>H<sub>90</sub>N<sub>8</sub>Pd<sub>4</sub>+H]<sup>+</sup> m/z = 1997.3554. IR: 2089 cm<sup>-1</sup> v(C≡C).

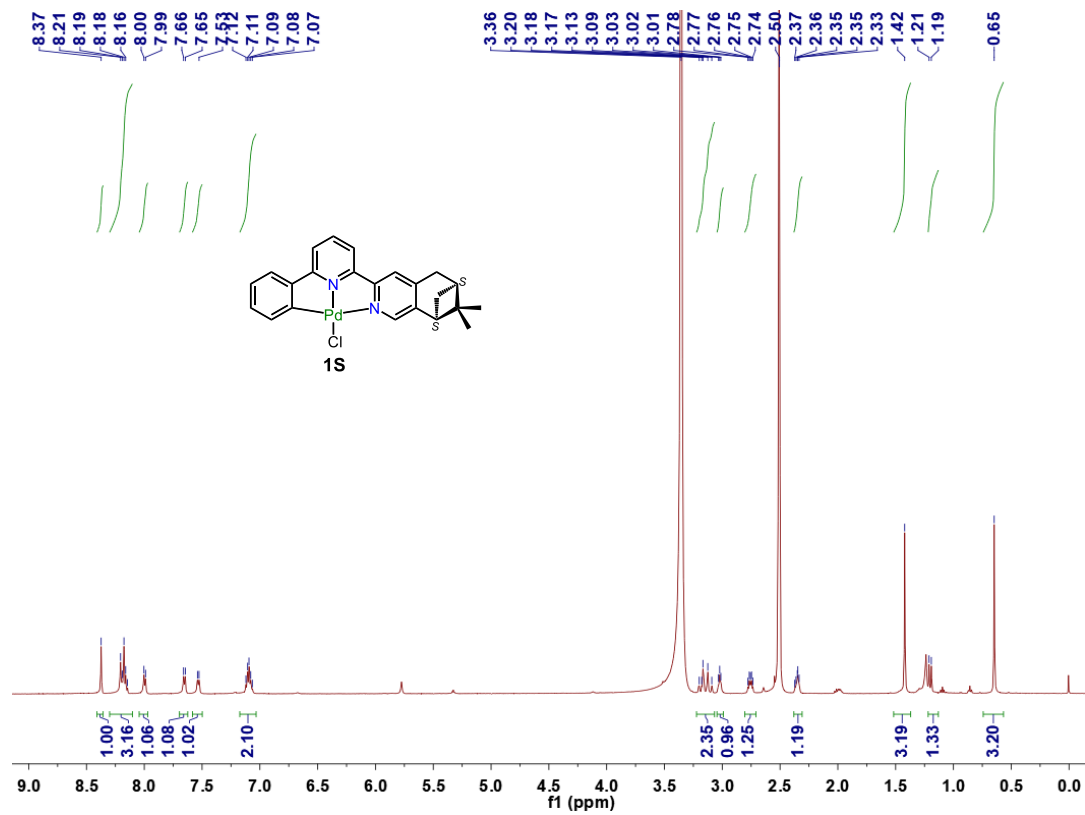
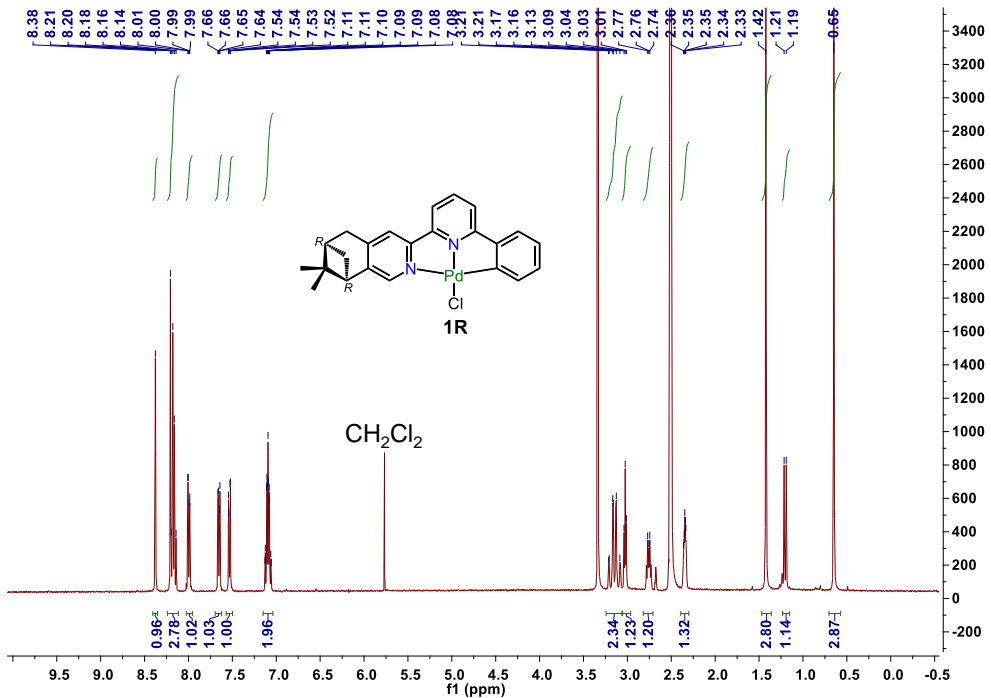
**Table S1.** Crystal Data for **3M** and **3P**.

	<b>3M·CHCl<sub>3</sub>·Et<sub>2</sub>O</b>	<b>3P·CHCl<sub>3</sub>·Et<sub>2</sub>O</b>
formula	C <sub>68.22</sub> H <sub>58.66</sub> Cl <sub>3.78</sub> N <sub>4</sub> O <sub>0.74</sub> Pd <sub>2</sub>	C <sub>68.02</sub> H <sub>58.06</sub> Cl <sub>3.98</sub> N <sub>4</sub> O <sub>0.67</sub> Pd <sub>2</sub>
fw	1293.13	1296.14
colour	orange	orange
crystal size	0.32×0.2×0.09	0.39×0.16×0.14
crystal system	hexagonal	trigonal
space group	P6 <sub>2</sub>	P3 <sub>1</sub>
<i>a</i> , Å	20.5184(11)	20.5118(14)
<i>b</i> , Å	20.5184(11)	20.5118(14)
<i>c</i> , Å	13.0844(7)	13.0966(10)
$\alpha$ , deg	90	90
$\beta$ , deg	90	90
$\gamma$ , deg	120	120
<i>V</i> , Å <sup>3</sup>	4770.6(6)	4772.0(7)
<i>Z</i>	3	3
<i>D<sub>c</sub></i> , g cm <sup>-3</sup>	1.350	1.353
$\mu$ , mm <sup>-1</sup>	0.768	0.776
<i>F</i> (000)	1974.0	1978.0
2 <i>θ</i> <sub>max</sub> , deg	50.78	46.53
no. reflections	38611	32825
no. independent reflections	5835 [ <i>R</i> (int) = 0.0609]	8818 [ <i>R</i> (int) = 0.0782]
no. variables	477	974
<i>GOF</i> on F <sup>2</sup>	1.090	1.047
Flack parameter	0.02(4)	0.09(3)
<i>R</i> <sub>1</sub> <sup>a</sup> [ <i>I</i> >2σ( <i>I</i> )]	0.0818	0.0591
<i>wR</i> <sub>2</sub> <sup>b</sup>	0.2120	0.1480
residual <i>ρ</i> , eÅ <sup>-3</sup>	+1.66, -1.02	+0.65, -0.45

<sup>a</sup> *R* = Σ||F<sub>o</sub>|−|F<sub>c</sub>||/Σ|F<sub>o</sub>|. <sup>b</sup> *Rw* = {Σ[w(F<sub>o</sub><sup>2</sup>−F<sub>c</sub><sup>2</sup>)<sup>2</sup>]/Σ[w(F<sub>o</sub><sup>2</sup>)<sup>2</sup>]}<sup>1/2</sup>

**Table S2** Photoluminescence data of complexes **2S/2R**, **3M/3P** and **4M/4P**.

	Medium	T / K	$\lambda_{\text{em,max}} / \text{nm}$ ( $\tau_{\text{em}} / \mu\text{s}$ )	$\Phi_{\text{em}}$	$k_r / \text{s}^{-1}$	$g_{\text{lum}}$
<b>2R</b>	Crystalline	298	417; 625 (1.2)	<1%		
		77	546 (420)			
	CH <sub>2</sub> Cl <sub>2</sub>	298	Non-emissive			
	2-MeTHF	77	477 (65.0)			
<b>2S</b>	Crystalline	298	417; 625 (1.2)	<1%		
		77	556 (398)			
	CH <sub>2</sub> Cl <sub>2</sub>	298	Non-emissive			
	2-MeTHF	77	477 (65.0)			
<b>3M</b>	Crystalline	298	652 (1.2)	10%		
		77	673 (11.7)			
	CH <sub>2</sub> Cl <sub>2</sub>	298	642 (3.4)	50%	$1.5 \times 10^5$	$1 \times 10^{-3}$
	2-MeTHF	77	510 (939.4); 640 (11.7)			
<b>3P</b>	Crystalline	298	652 (1.3)	15%		
		77	673 (14.3)			
	CH <sub>2</sub> Cl <sub>2</sub>	298	642 (3.6)	54%	$1.3 \times 10^5$	$-1 \times 10^{-3}$
	2-MeTHF	77	510 (928.6); 640 (15.2)			
<b>4M</b>	Crystalline	298	656 (0.02)	<1%		
		77	670 (9.9)			
	CH <sub>2</sub> Cl <sub>2</sub>	298	647 (3.4)	41%	$1.2 \times 10^5$	$2 \times 10^{-3}$
	2-MeTHF	77	536 (105.2); 630 (13.7)			
<b>4P</b>	Crystalline	298	670 (0.02)	<1%		
		77	665 (6.3)			
	CH <sub>2</sub> Cl <sub>2</sub>	298	647 (3.5)	43%	$1.2 \times 10^5$	$-2 \times 10^{-3}$
	2-MeTHF	77	536 (101.6); 630 (13.6)			



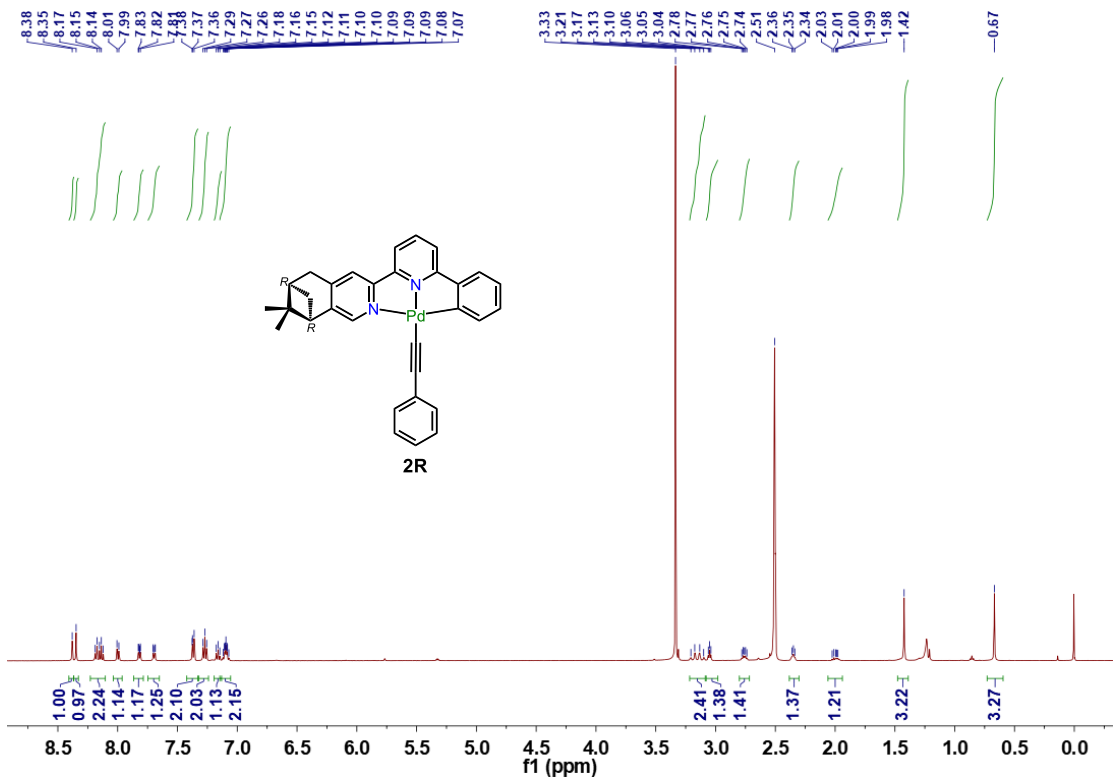


**Figure S3.**  $^1\text{H}$  NMR spectrum of **2R** in DMSO.

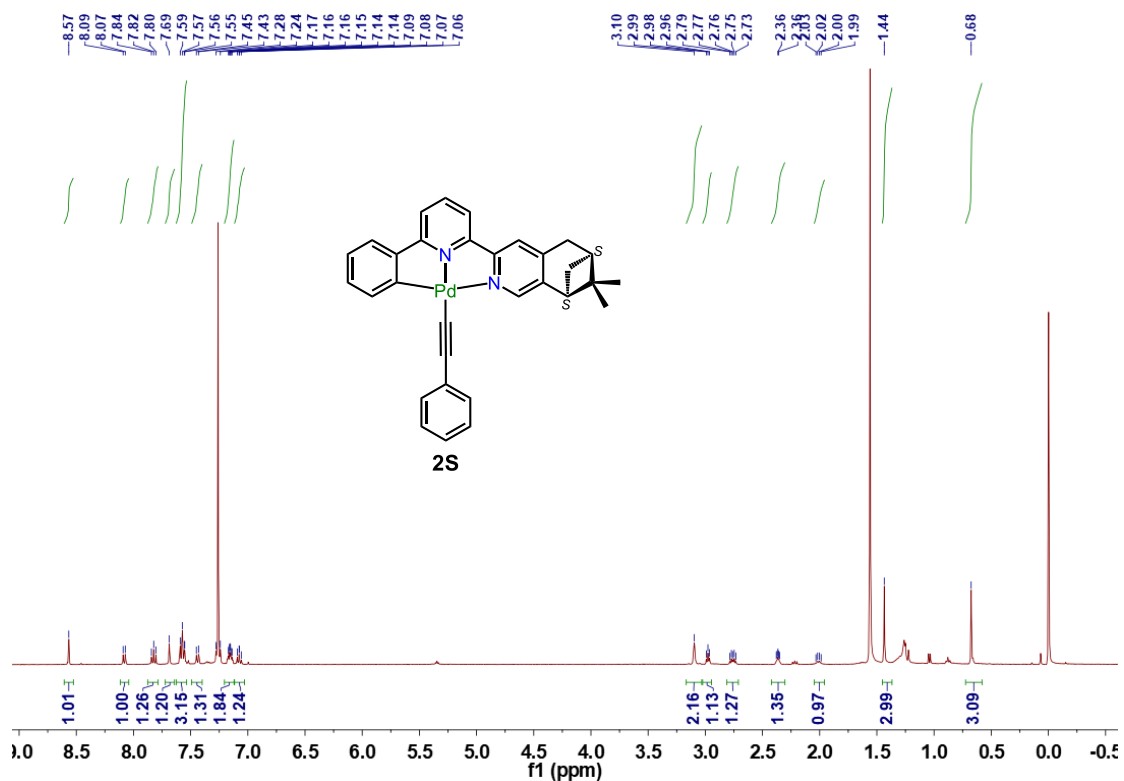


**Figure S4.**  $^1\text{H}$  NMR spectrum of **2S** in  $\text{CDCl}_3$ .

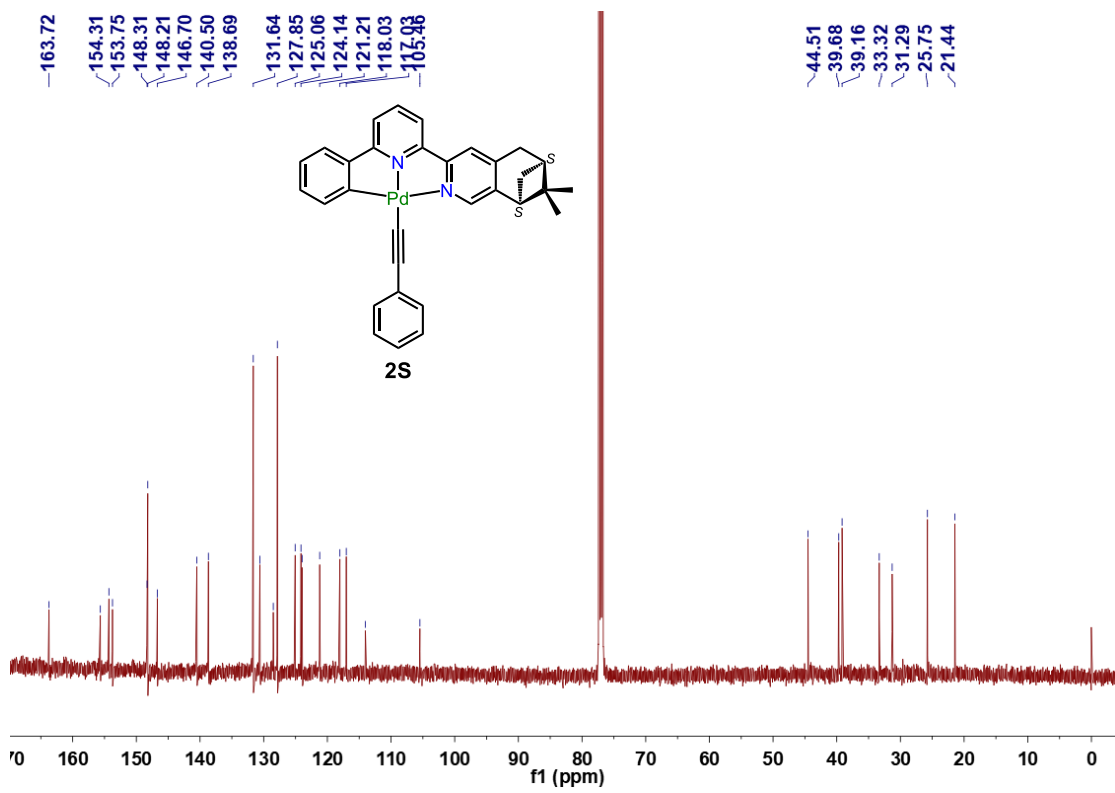


**Figure S5.**  $^{13}\text{C}$  NMR spectrum of **2S** in  $\text{CDCl}_3$ .

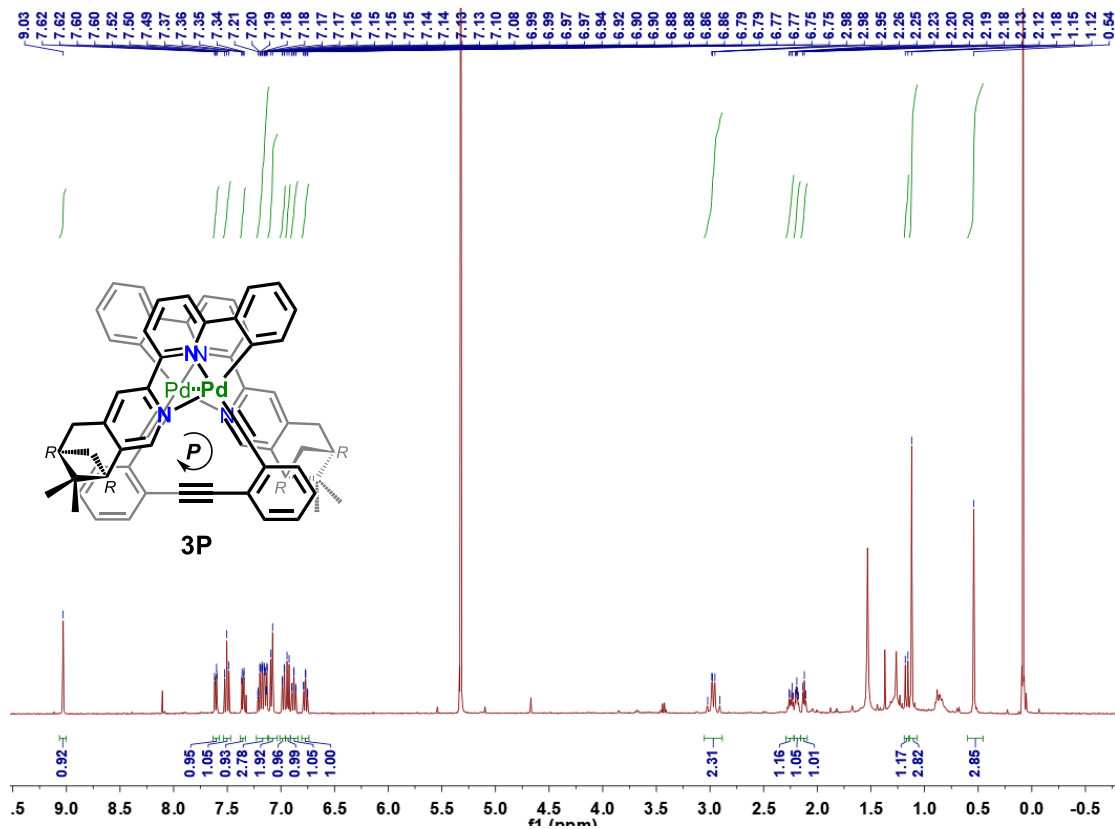


**Figure S6.**  $^1\text{H}$  NMR spectrum of **3P** in  $\text{CD}_2\text{Cl}_2$ .

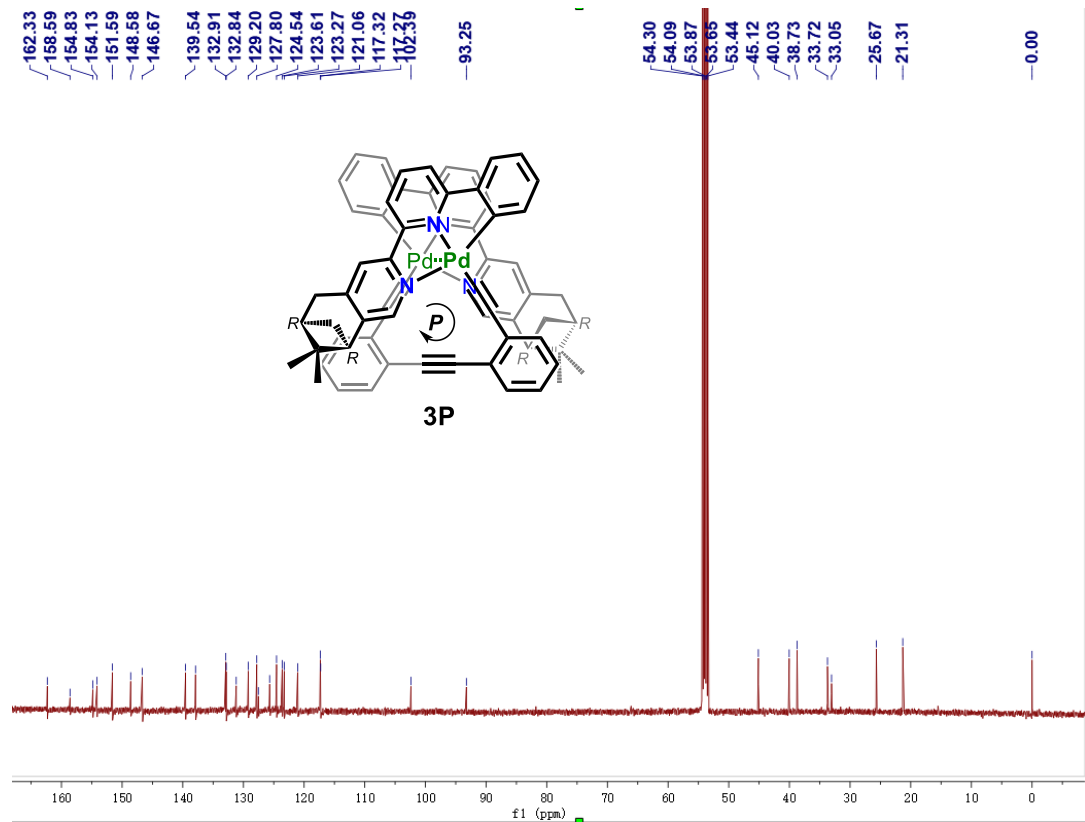


**Figure S7.**  $^{13}\text{C}$  NMR spectrum of **3P** in  $\text{CD}_2\text{Cl}_2$ .

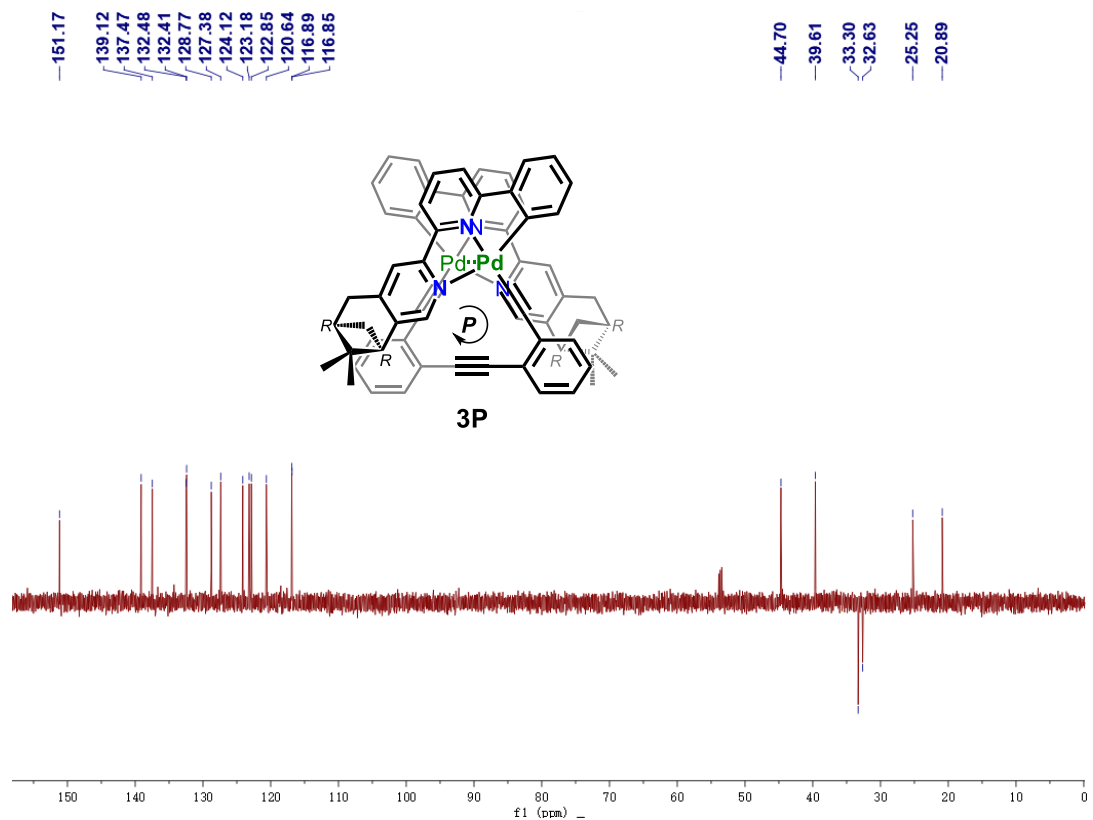


**Figure S8.** DEPT 135 NMR spectrum of **3P** in  $\text{CD}_2\text{Cl}_2$ .

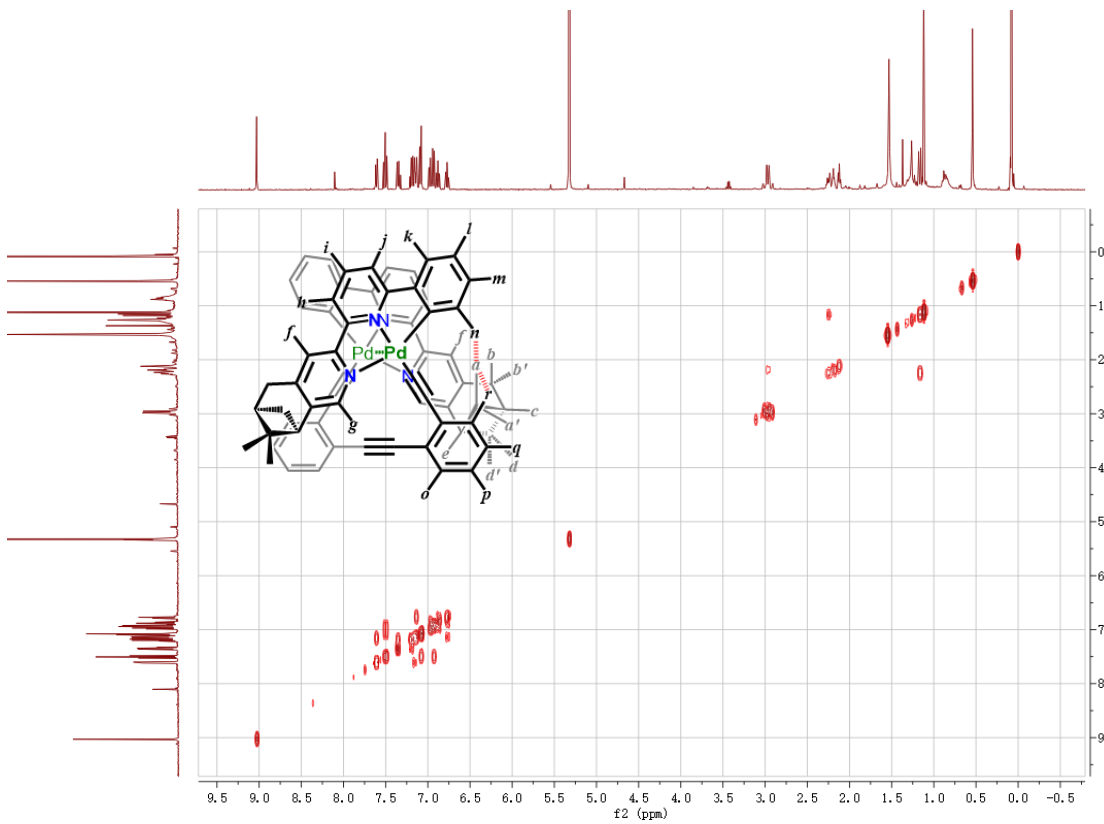


**Figure S9.**  $^1\text{H}$ - $^1\text{H}$  COSY NMR spectrum of **3P** in  $\text{CD}_2\text{Cl}_2$ .

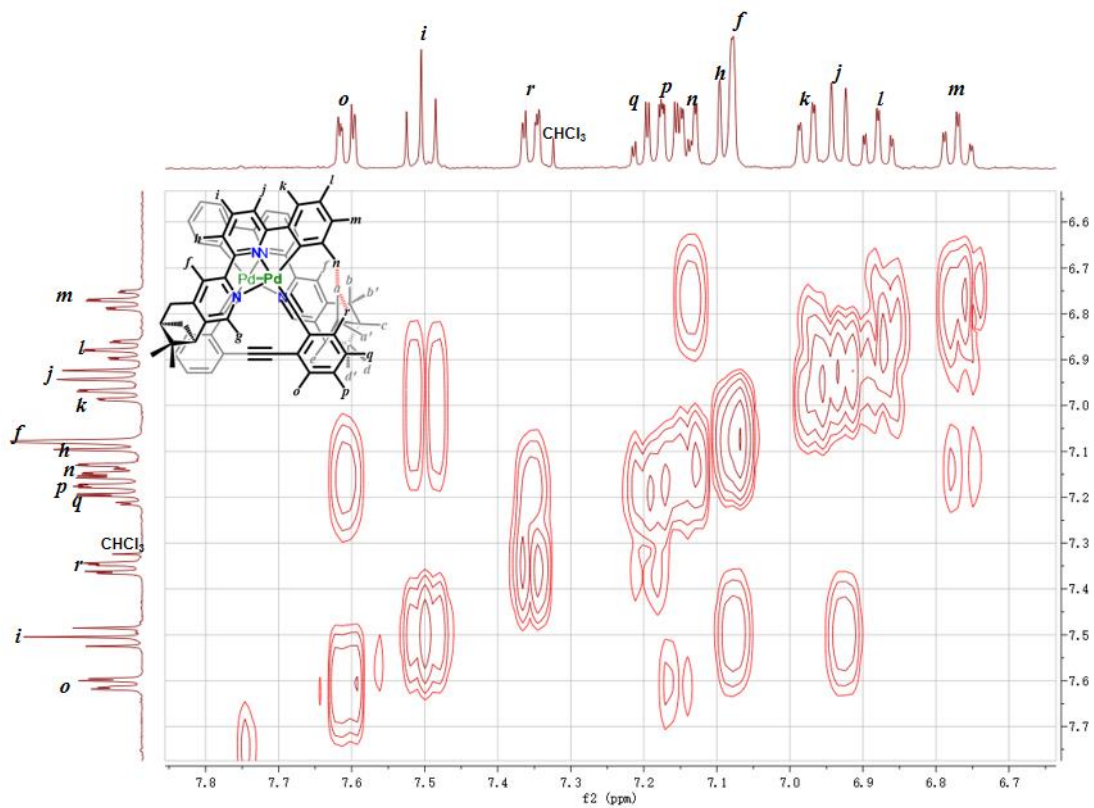


**Figure S10.** Partial  $^1\text{H}$ - $^1\text{H}$  COSY NMR spectrum of **3P** in  $\text{CD}_2\text{Cl}_2$ .

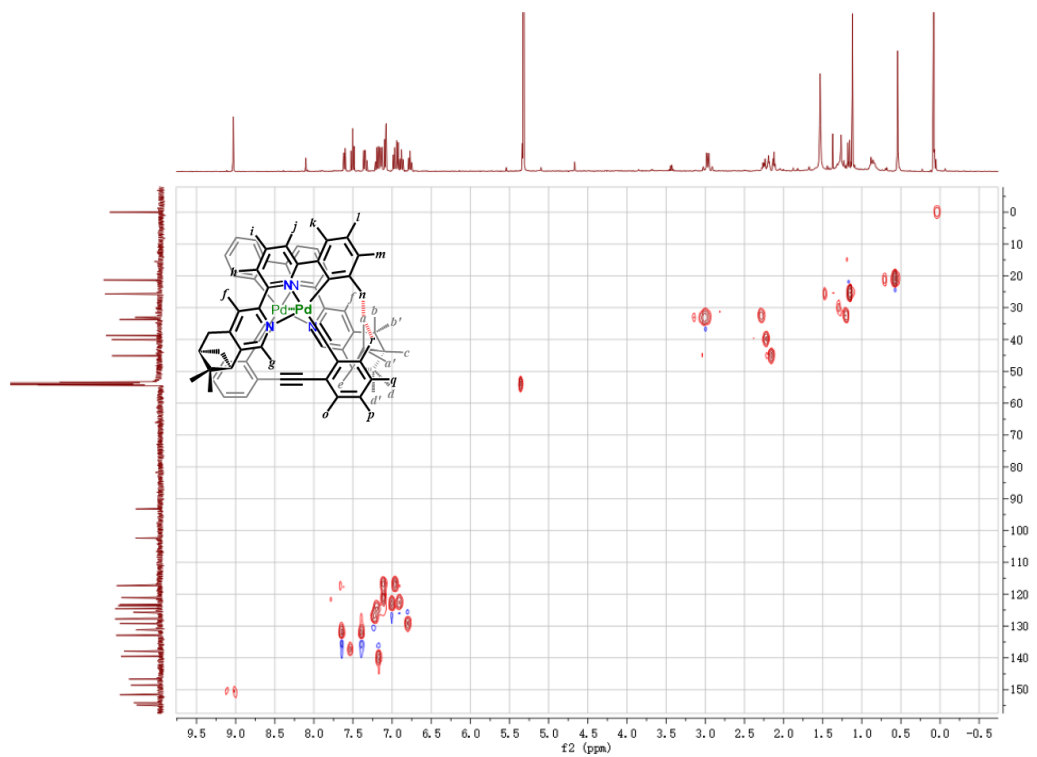


**Figure S11.**  $^{13}\text{C}$ - $^1\text{H}$  HSQC NMR spectrum of **3P** in  $\text{CD}_2\text{Cl}_2$ .

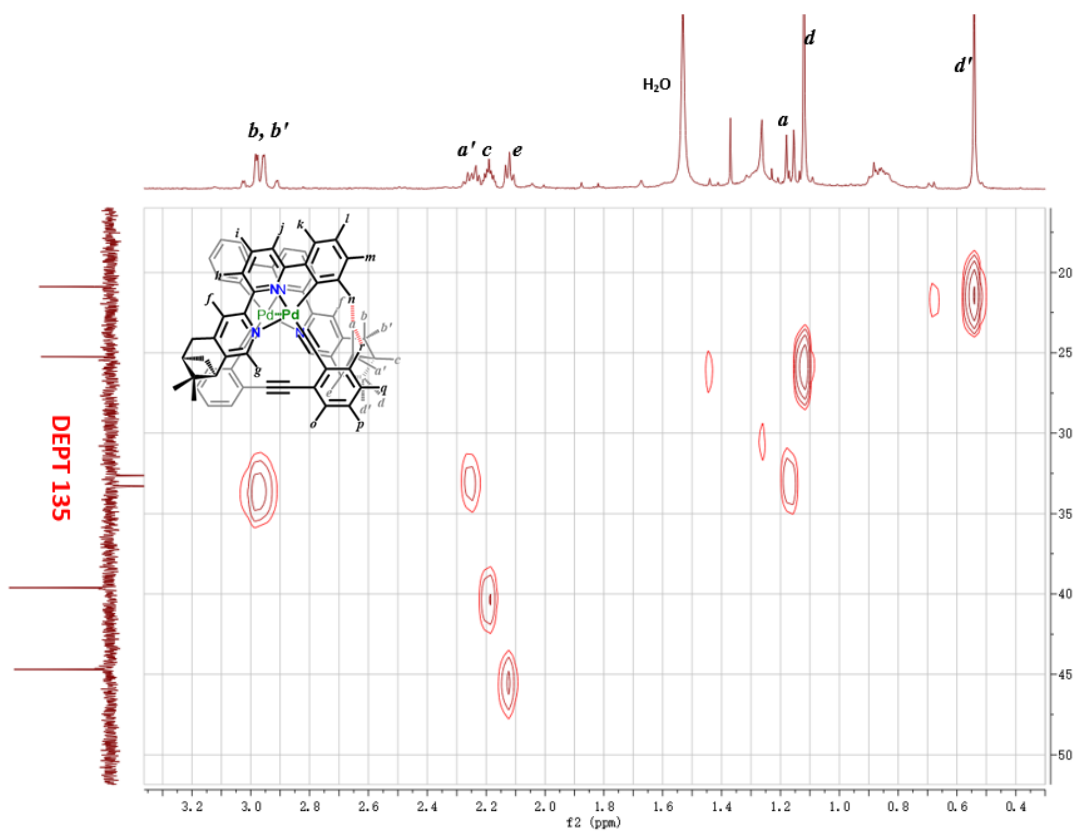


**Figure S12.** Partial  $^{13}\text{C}$ - $^1\text{H}$  HSQC NMR spectrum of **3P** in  $\text{CD}_2\text{Cl}_2$ .

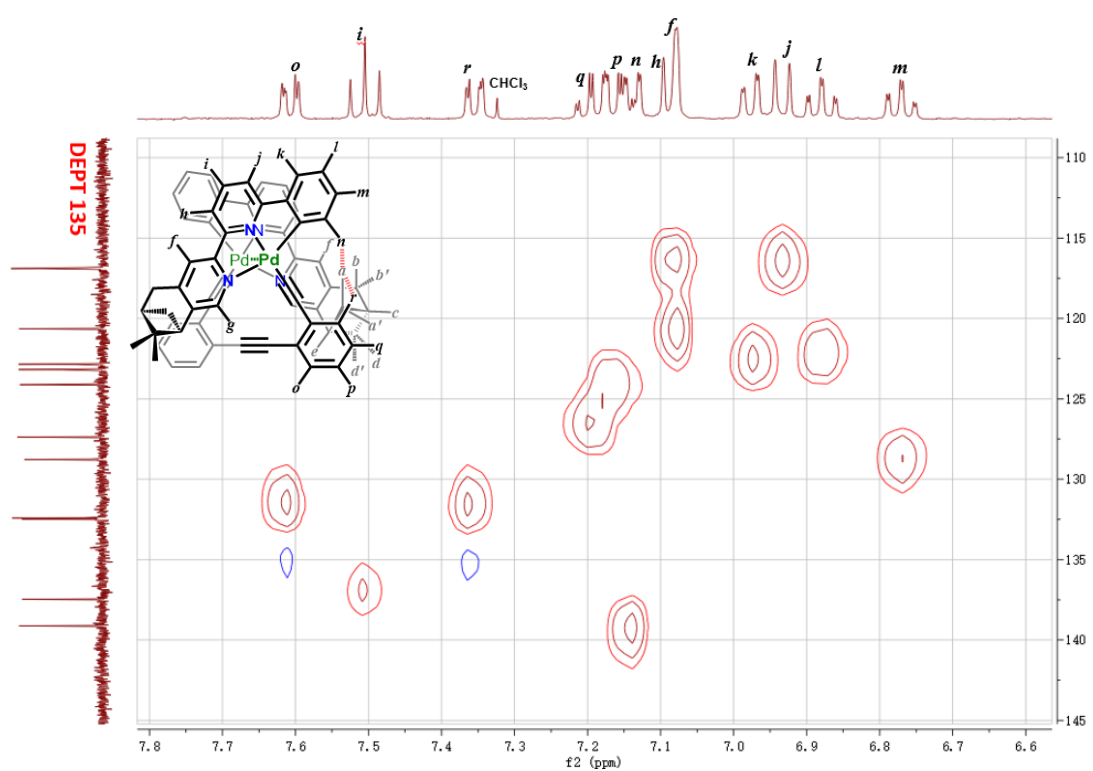


**Figure S13.** Partial  $^{13}\text{C}$ - $^1\text{H}$  HSQC NMR spectrum of **3P** in  $\text{CD}_2\text{Cl}_2$ .

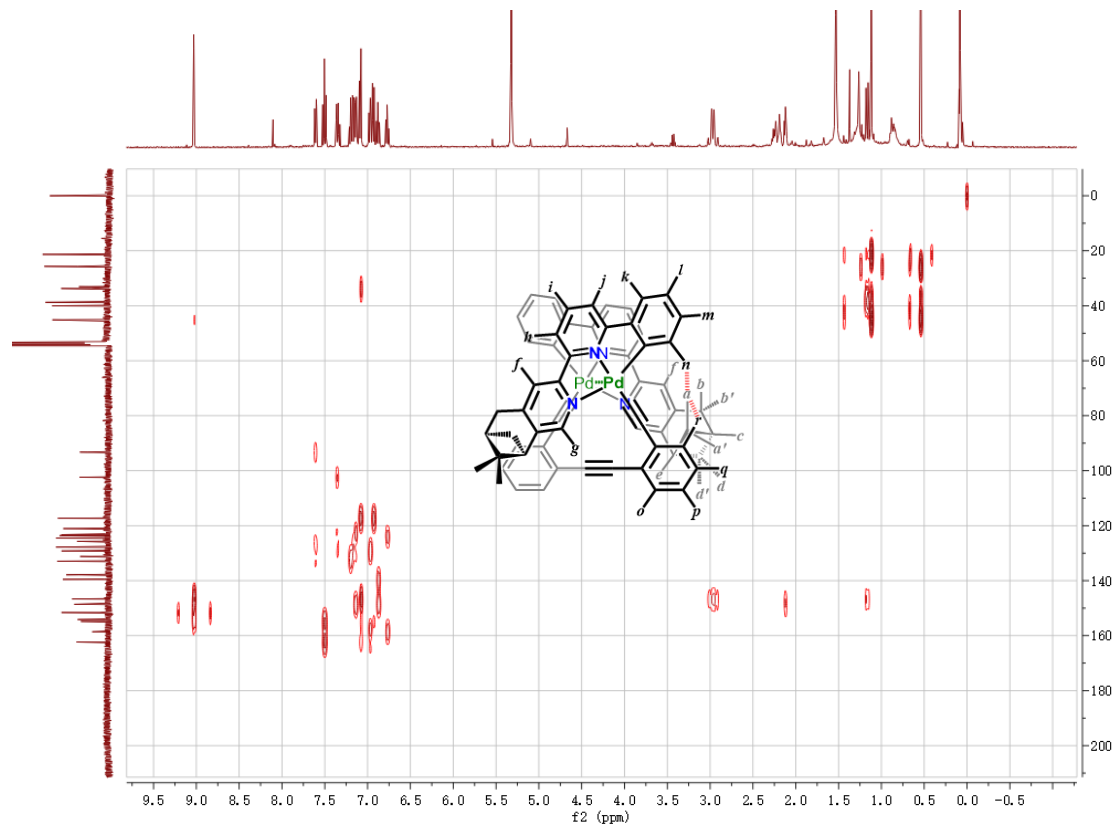


**Figure S14.**  $^{13}\text{C}$ - $^1\text{H}$  HMBC NMR spectrum of **3P** in  $\text{CD}_2\text{Cl}_2$ .

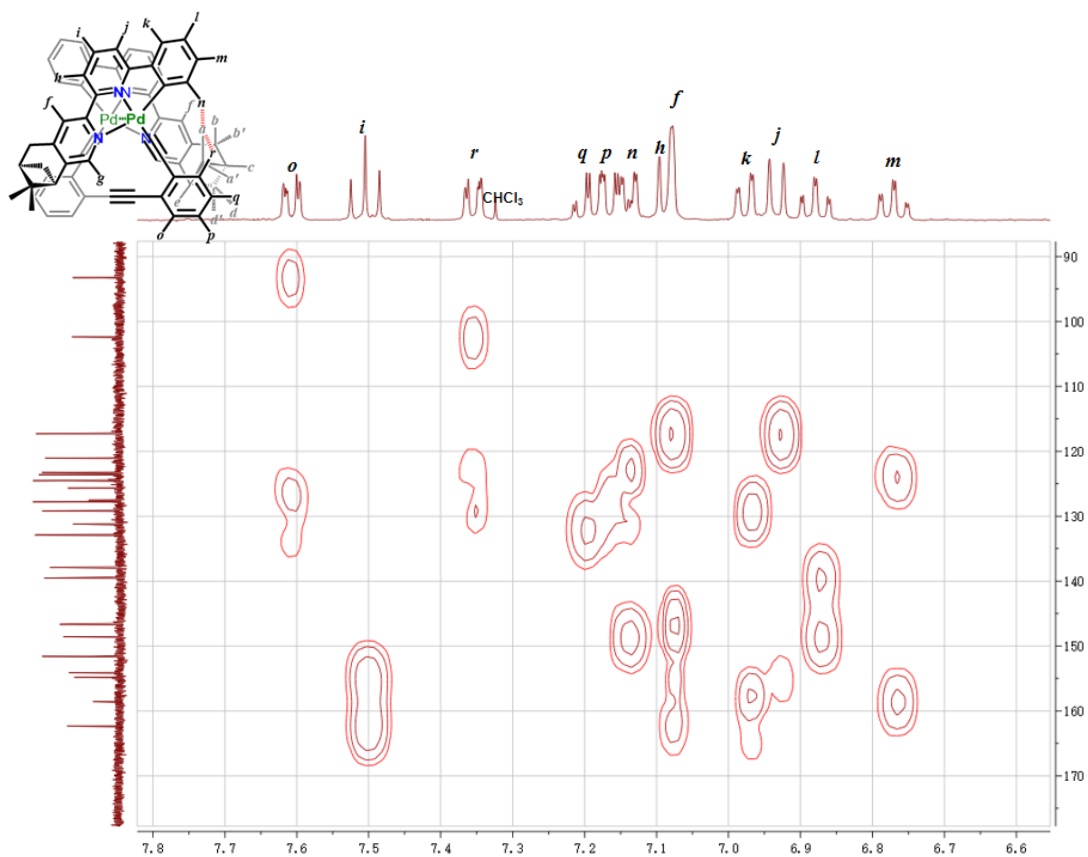


**Figure S15.** Partial  $^{13}\text{C}$ - $^1\text{H}$  HMBC NMR spectrum of **3P** in  $\text{CD}_2\text{Cl}_2$ .

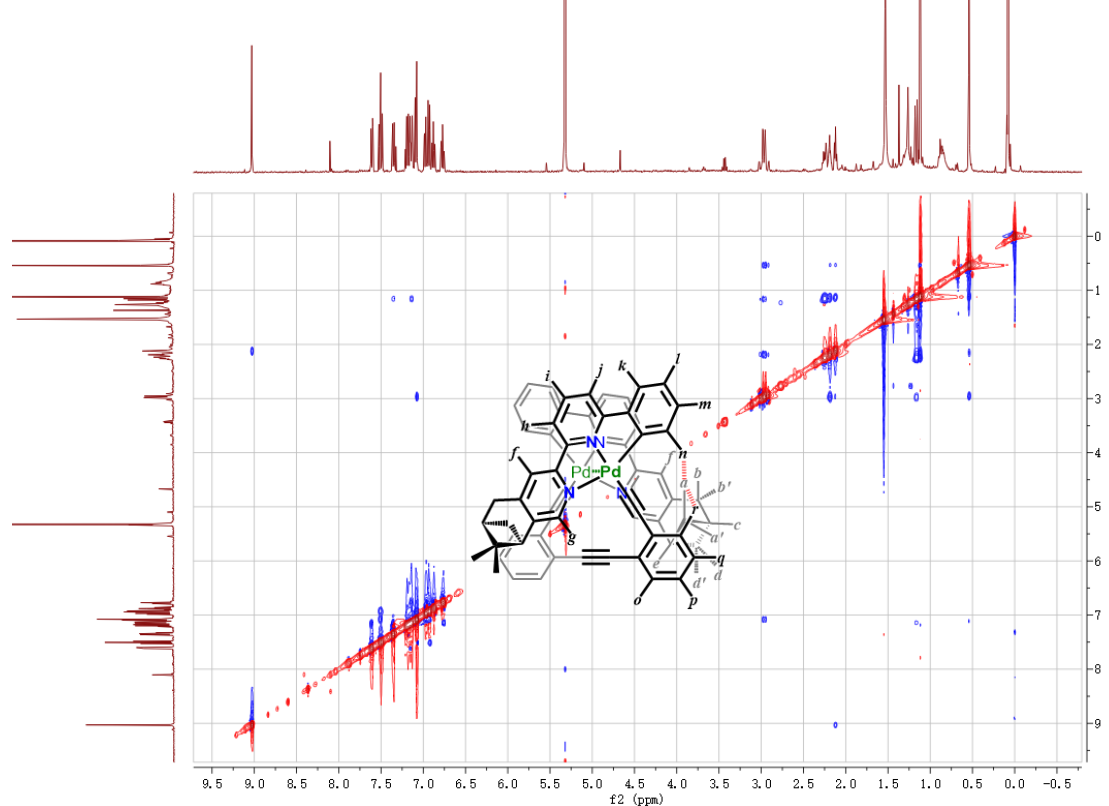


**Figure S16.**  $^1\text{H}$ - $^1\text{H}$  NOESY NMR spectrum of **3P** in  $\text{CD}_2\text{Cl}_2$ .

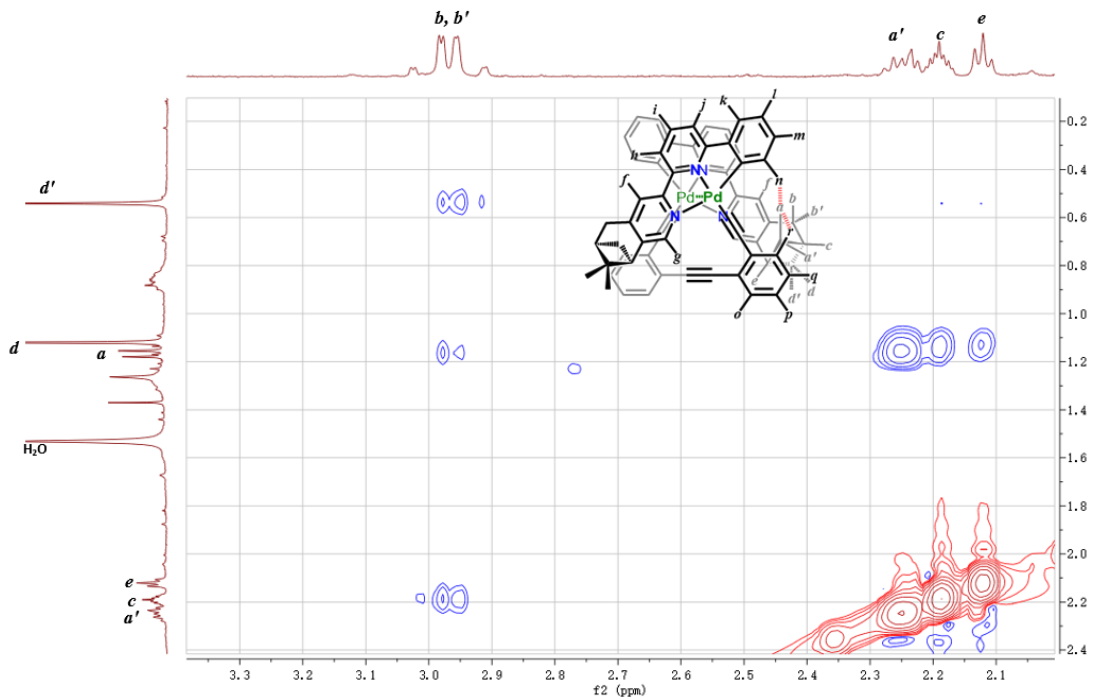


**Figure S17.** Partial  $^1\text{H}$ - $^1\text{H}$  NOESY NMR spectrum of **3P** in  $\text{CD}_2\text{Cl}_2$ .

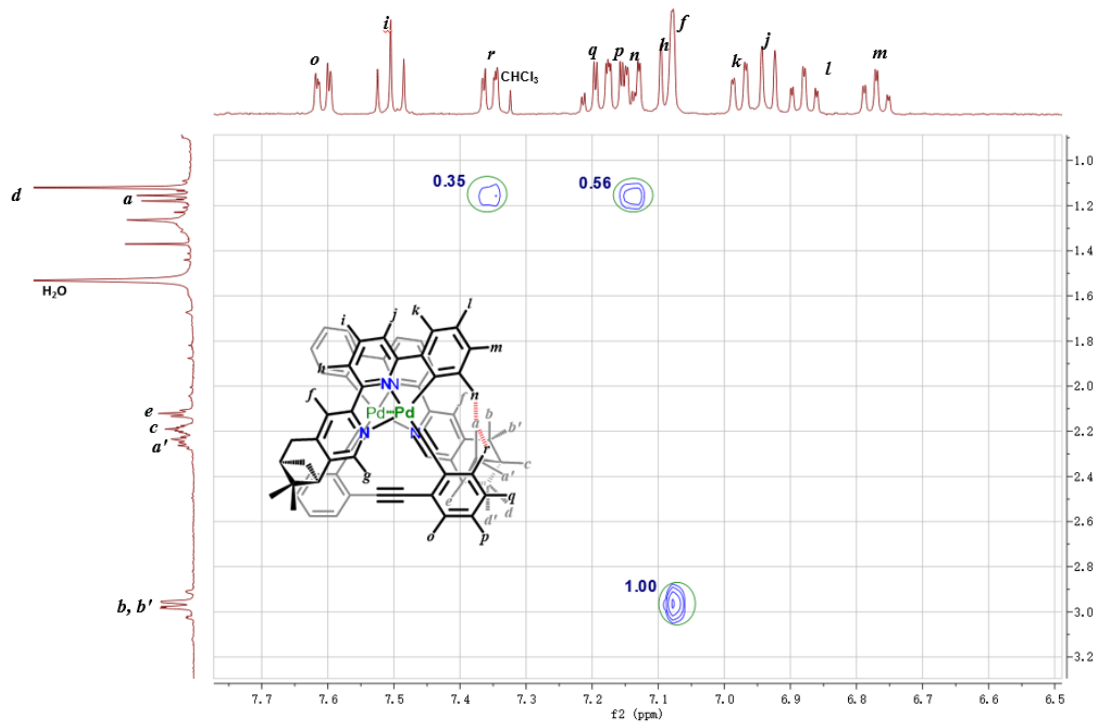


**Figure S18.** Partial  $^1\text{H}$ - $^1\text{H}$  NOESY NMR spectrum of **3P** in  $\text{CD}_2\text{Cl}_2$ .

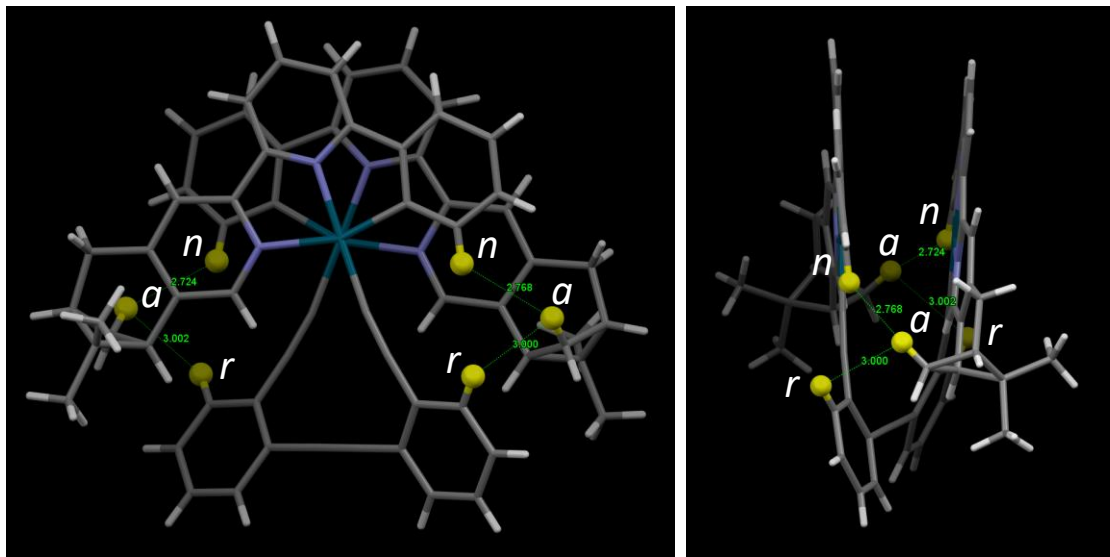


**Figure S19.** The spatial proximities between protons (*a*) and (*n* and *r*) in the crystal structure of **3P**·CHCl<sub>3</sub>·Et<sub>2</sub>O.

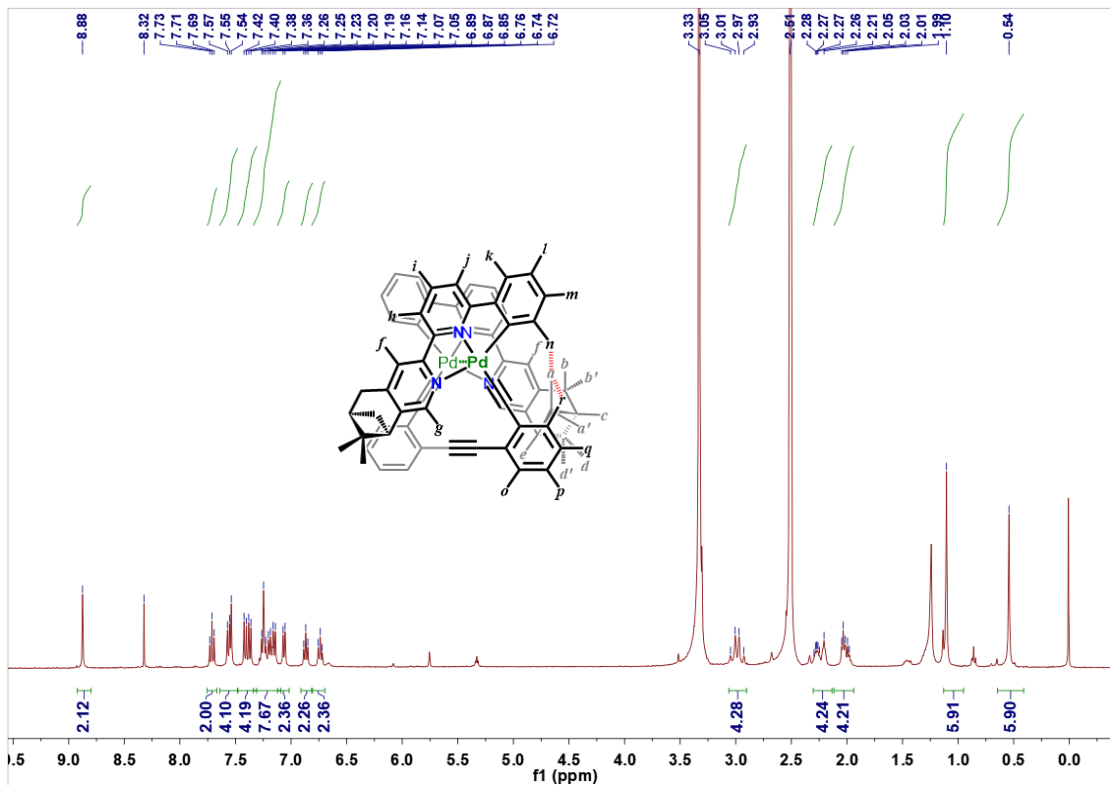


**Figure S20.** <sup>1</sup>H NMR spectrum of **3P** in DMSO.

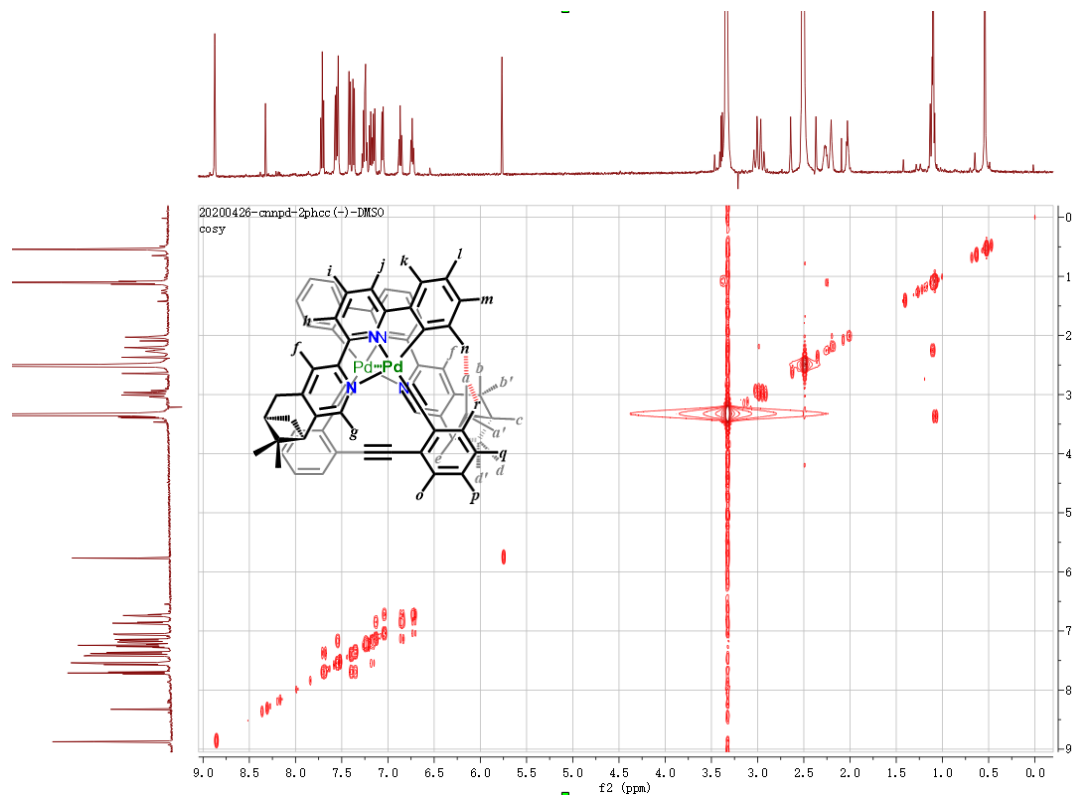


**Figure S21.**  $^1\text{H}$ - $^1\text{H}$  COSY NMR spectrum of **3P** in DMSO.

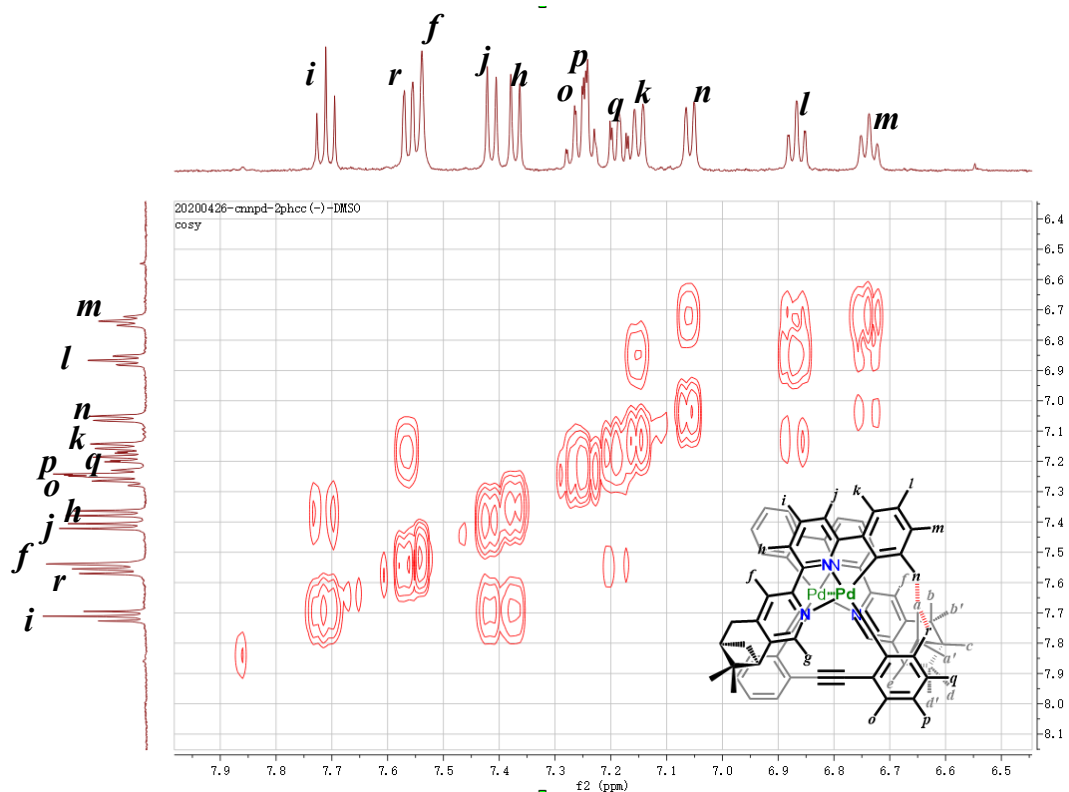


**Figure S22.** Partial  $^1\text{H}$ - $^1\text{H}$  COSY NMR spectrum of **3P** in DMSO.

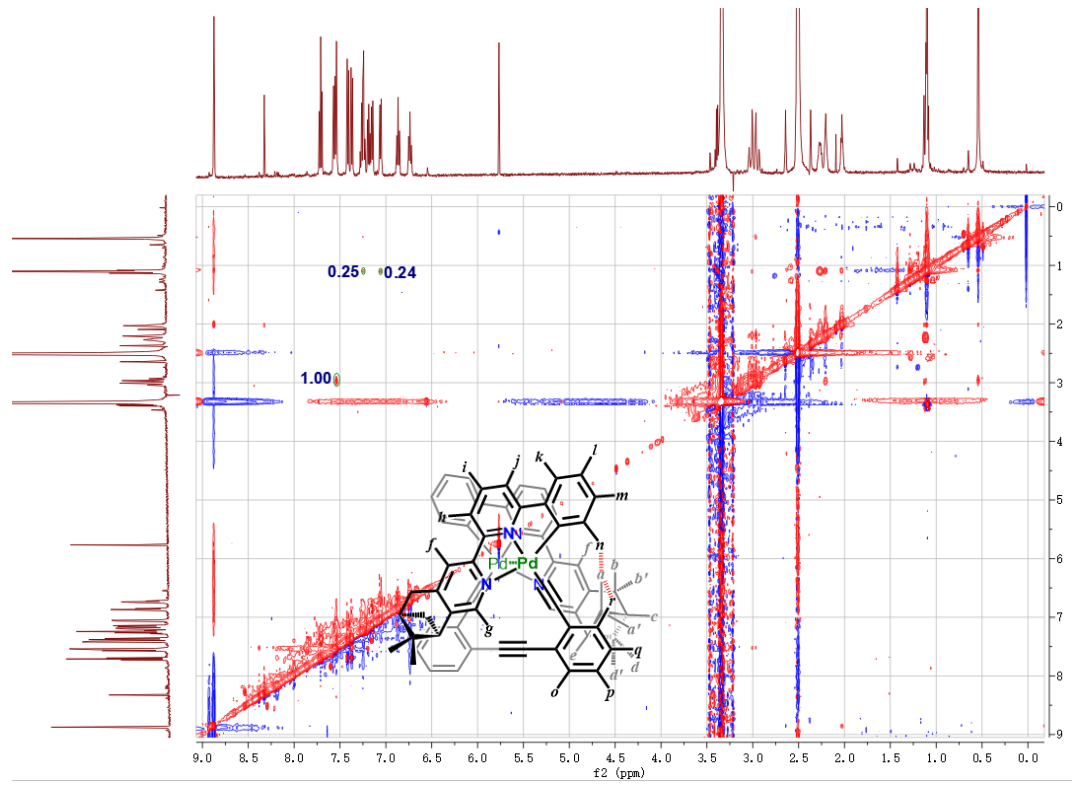


**Figure S23.**  $^1\text{H}$ - $^1\text{H}$  NOESY NMR spectrum of **3P** in DMSO.

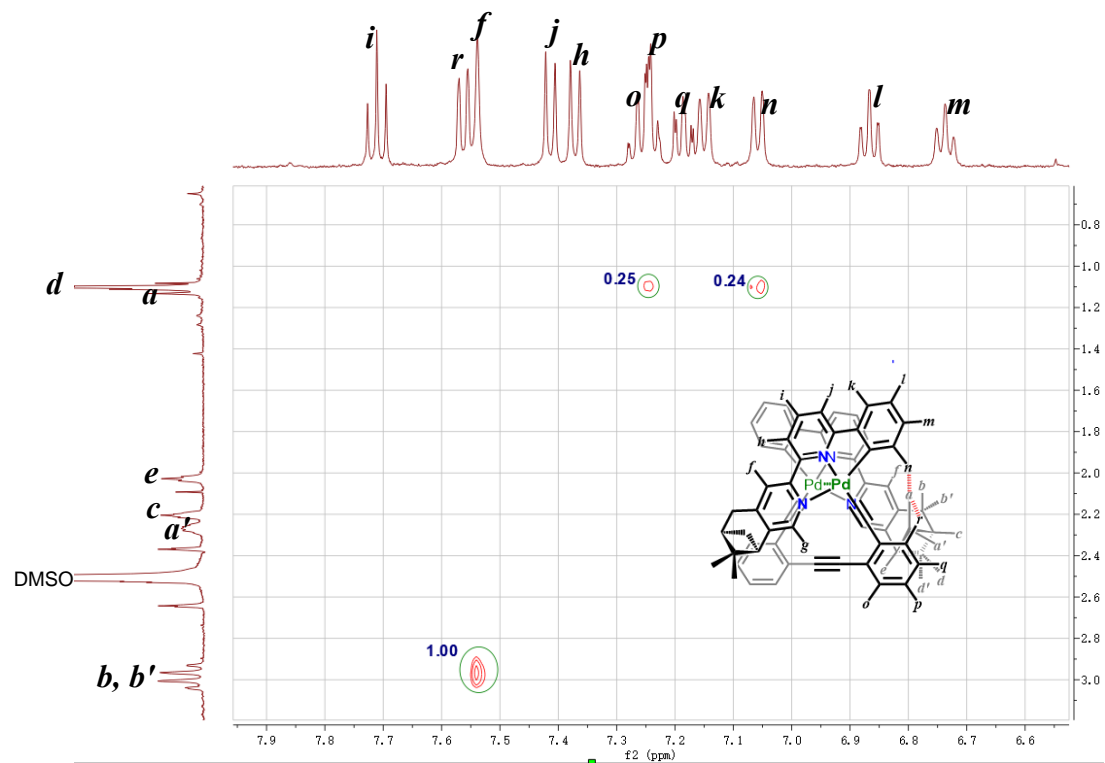


**Figure S24.** Partial  $^1\text{H}$ - $^1\text{H}$  NOESY NMR spectrum of **3P** in DMSO.

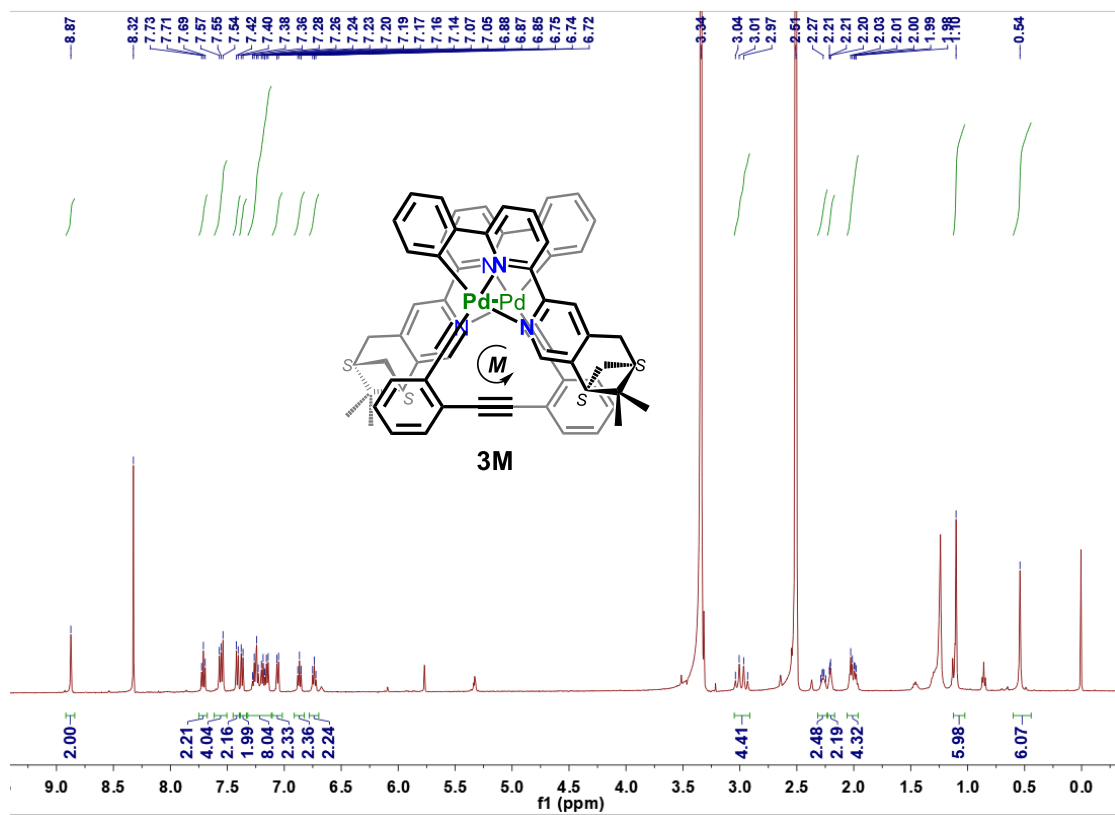


**Figure S25.**  $^1\text{H}$  NMR spectrum of **3M** in DMSO.

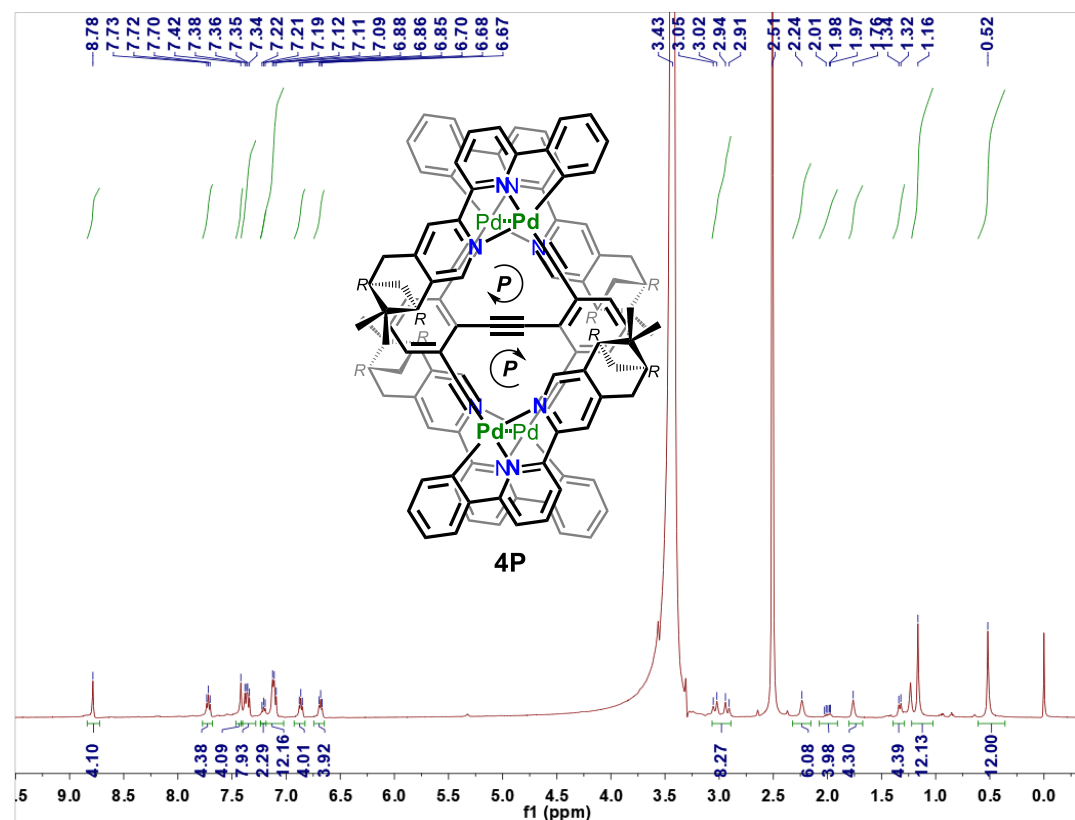


**Figure S26.**  $^1\text{H}$  NMR spectrum of **4P** in DMSO.

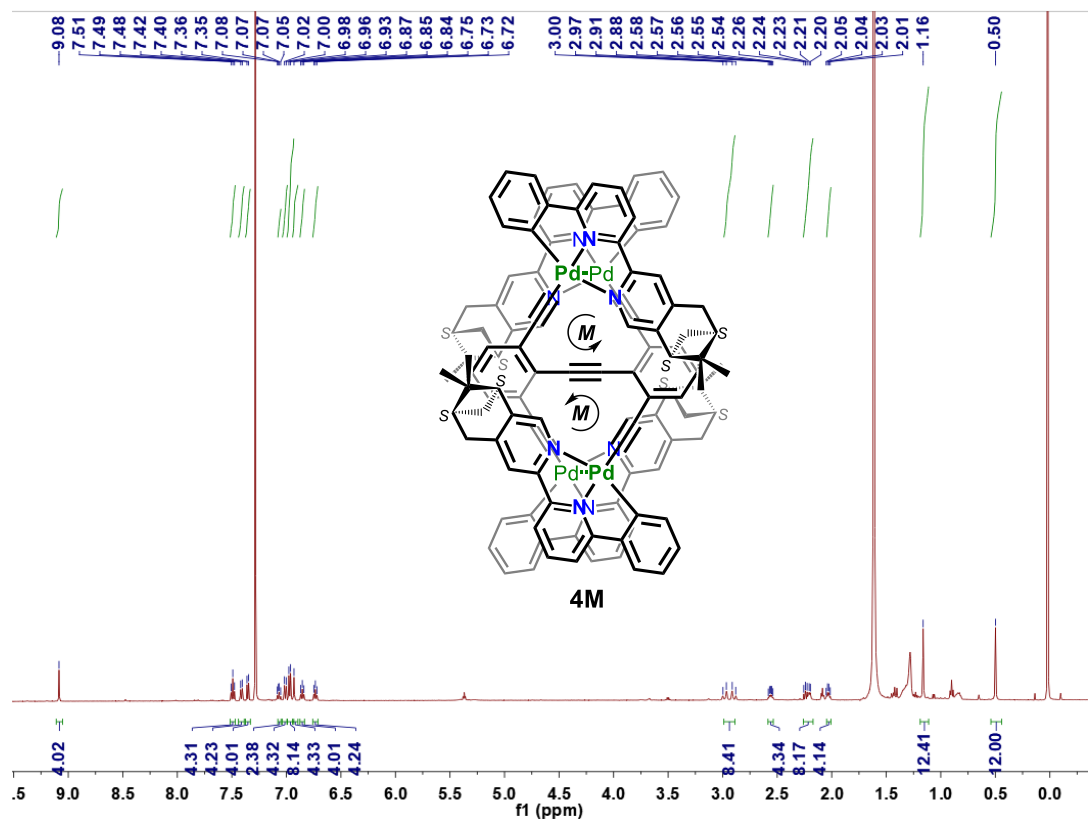


**Figure S27.**  $^1\text{H}$  NMR spectrum of **4M** in  $\text{CDCl}_3$ .

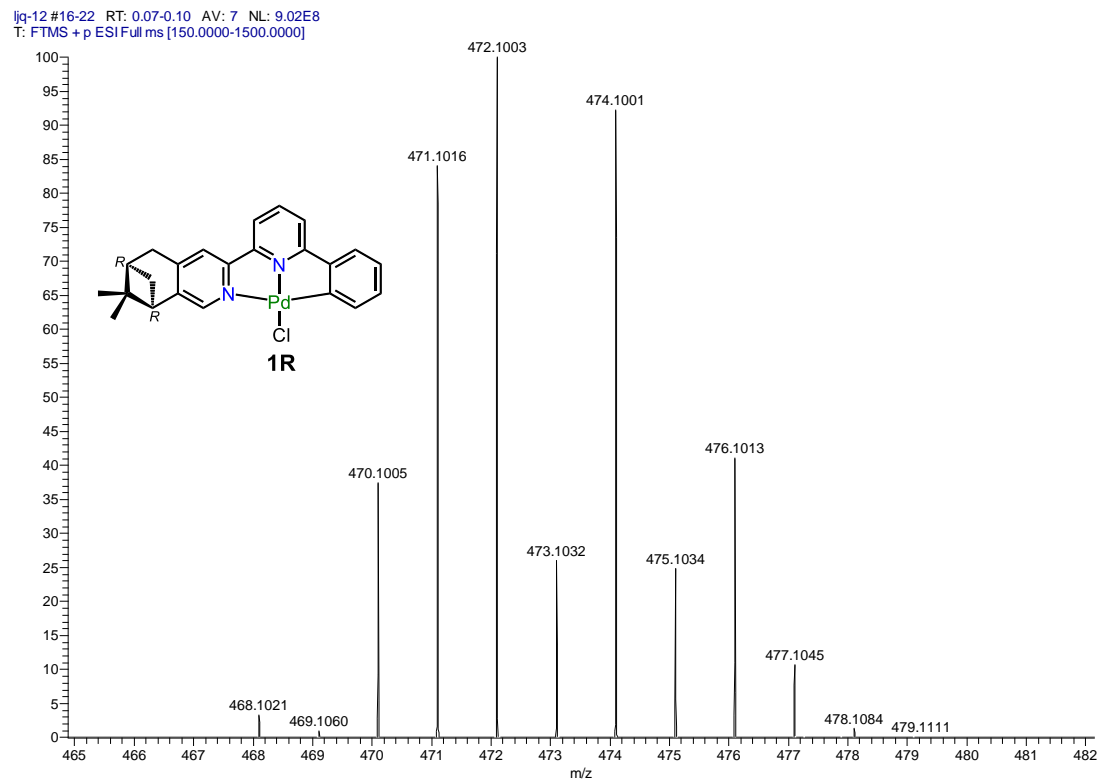


**Figure S28.** HR-MS spectrum of **1R**.

ljq-13 #16-20 RT: 0.07-0.09 AV: 5 NL: 7.89E8  
T: FTMS + p ESI Full ms [150.0000-1500.0000]

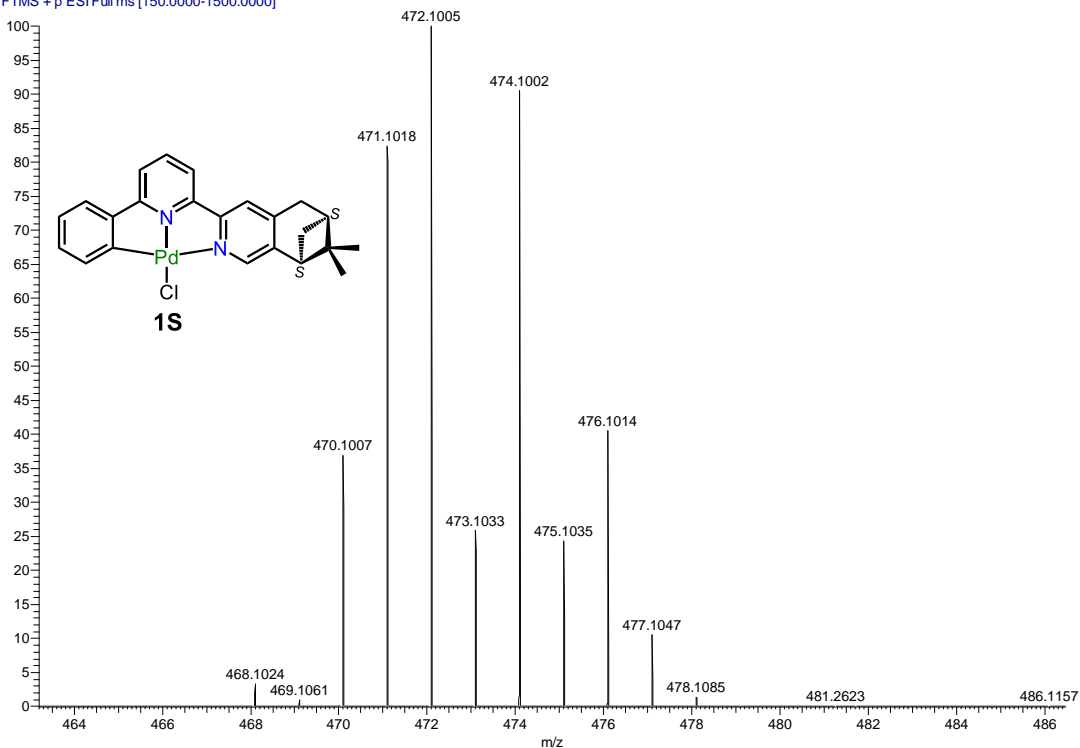


**Figure S29.** HR-MS spectrum of **1S**.

5-phcc-cnnpd(-) #14-22 RT: 0.06-0.10 AV: 9 NL: 3.88E6  
T: FTMS + p ESI Full ms [150.0000-2000.0000]

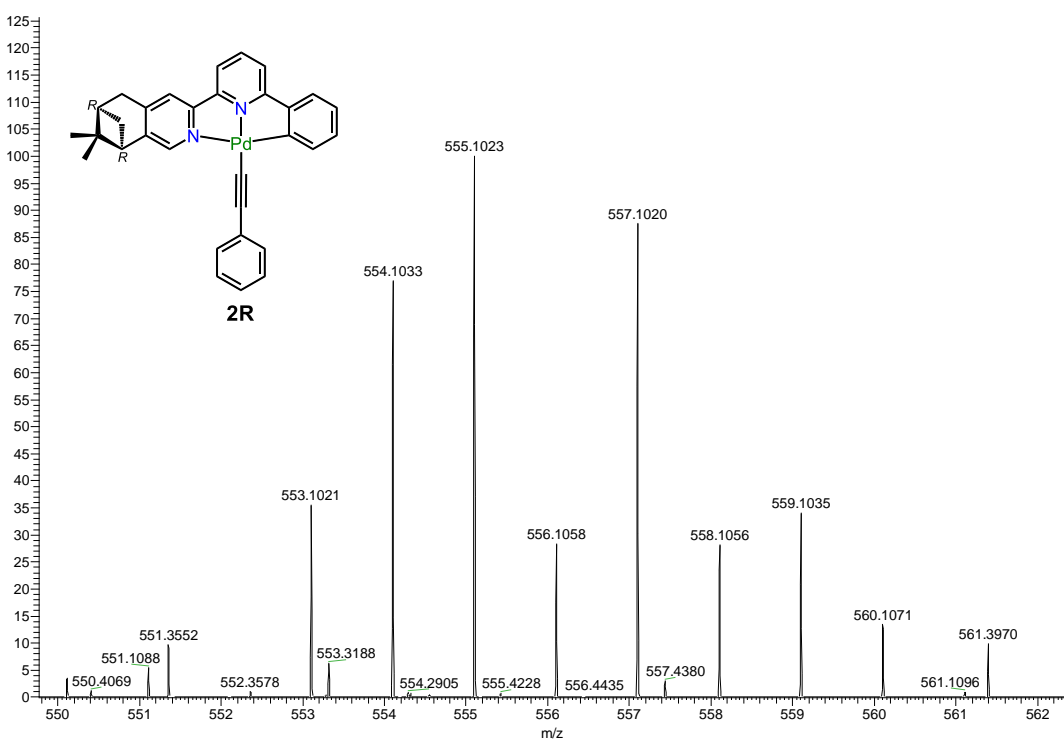


**Figure S30.** HR-MS spectrum of **2R**.

6-phcc-cnnpd(+) #17-29 RT: 0.07-0.13 AV: 13 NL: 5.71E6  
T: FTMS + p ESI Full ms [150.0000-2000.0000]

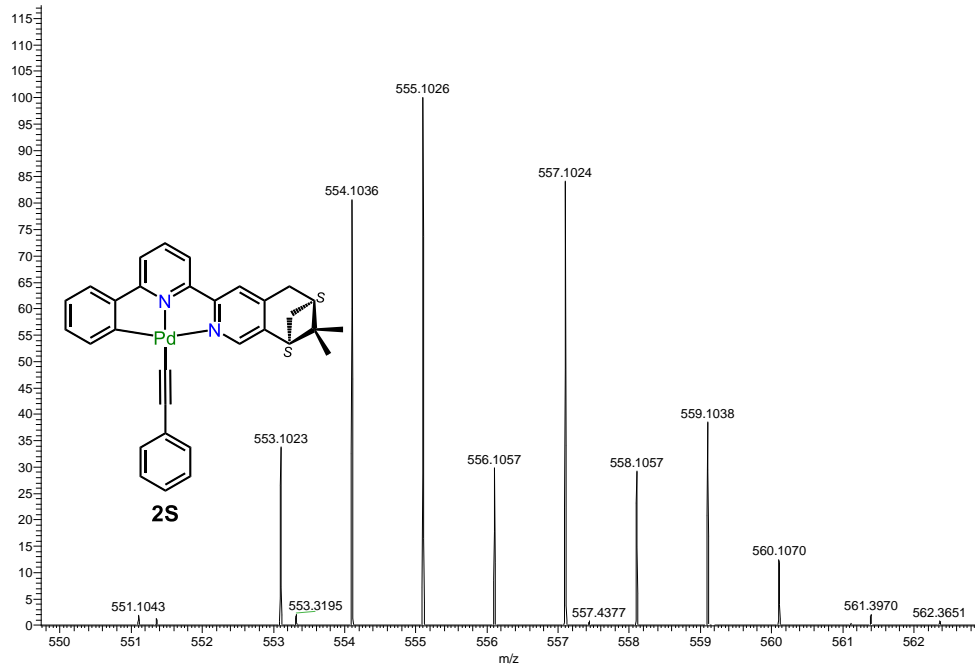


**Figure S31.** HR-MS spectrum of **2S**.

liq-10 #14-25 RT: 0.06-0.11 AV: 12 NL: 3.18E7  
T: FTMS + p ESI Full ms [150.0000-1500.0000]

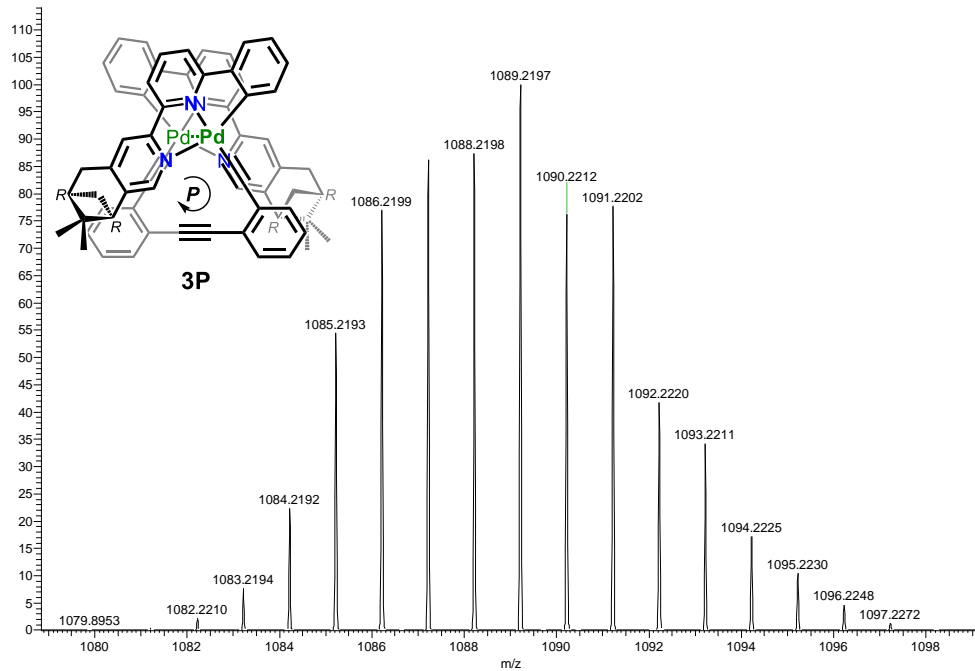


**Figure S32.** HR-MS spectrum of **3P**.

liq-11 #16-24 RT: 0.07-0.11 AV: 9 NL: 5.65E7  
T: FTMS + p ESI Full ms [150.0000-1500.0000]

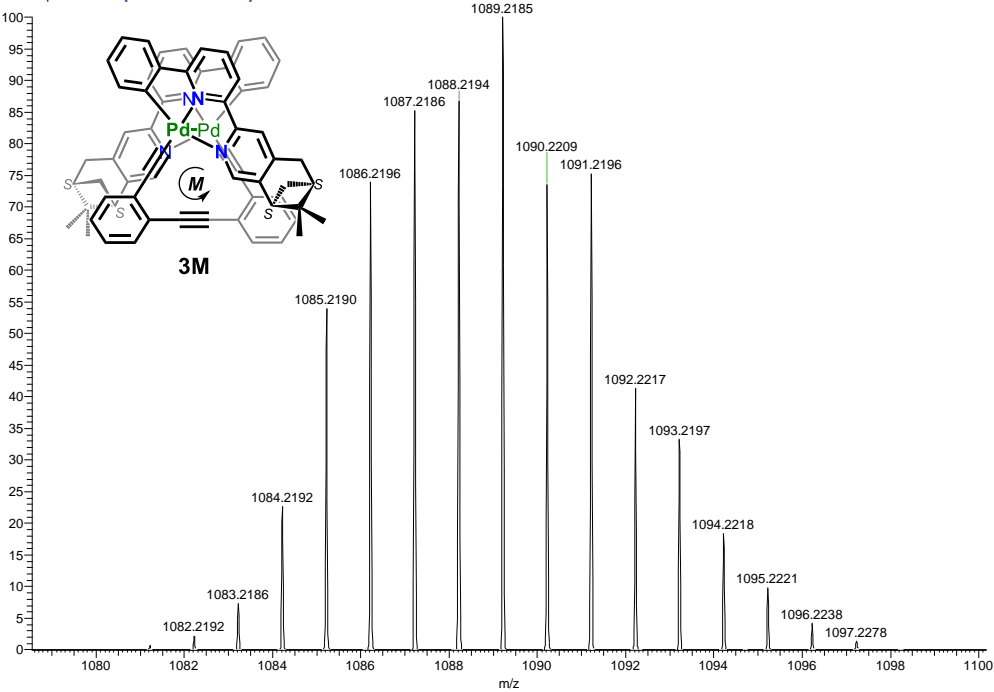


**Figure S33.** HR-MS spectrum of **3M**.

4CCPd( ) #15 RT: 0.17 AV: 1 NL: 2.25E5  
T: FTMS + p ESI Full ms [500.0000-2500.0000]

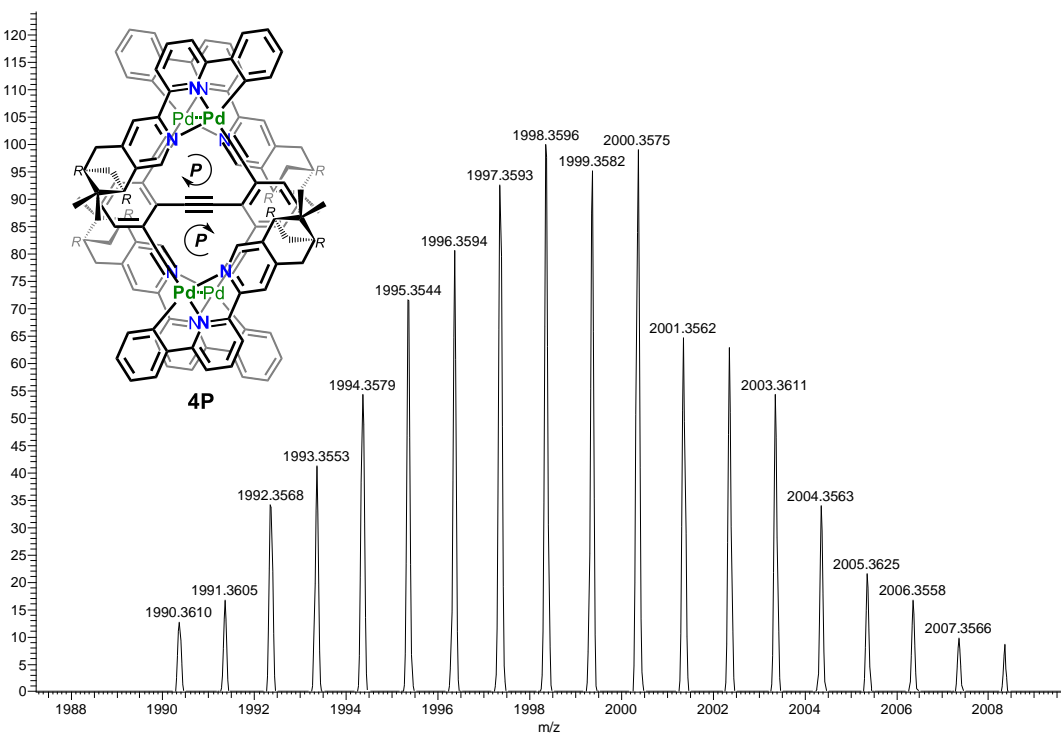


**Figure S34.** HR-MS spectrum of **4P**.

4ccpd(+) -right #9 RT: 0.08 AV: 1 NL: 4.47E6  
T: FTMS + p ESI Full ms [200.0000-3000.0000]

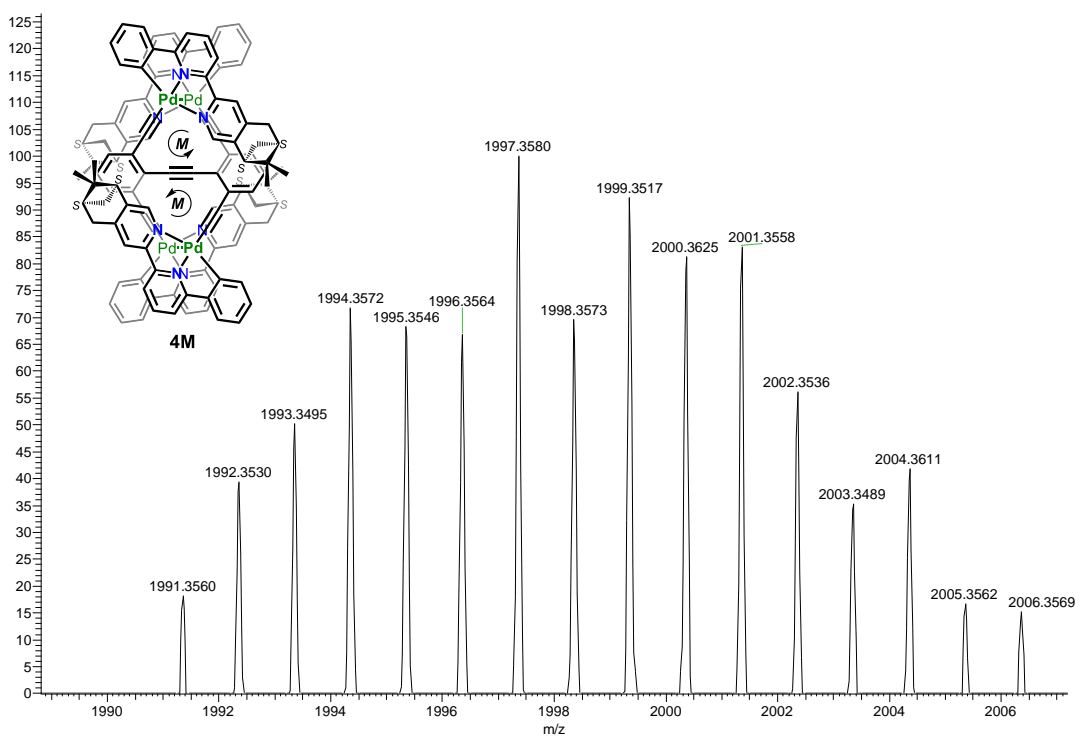


**Figure S35.** HR-MS spectrum of **4M**.

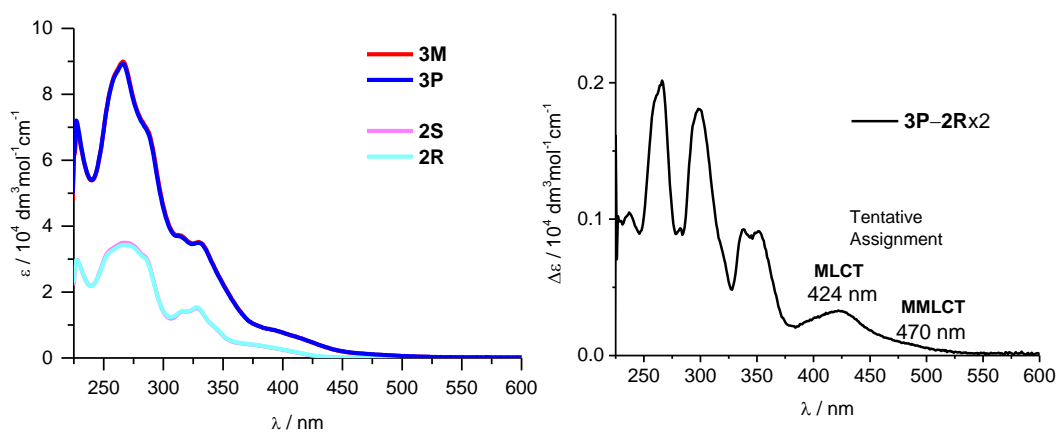


**Figure S36.** (left) UV-vis absorption spectra of **2S/2R** and **3M/3P** in  $\text{CH}_2\text{Cl}_2$  at 298 K. (right) The mathematic difference  $\Delta\varepsilon$  between **3P** and **2R** ( $\varepsilon$  values multiplied by 2).

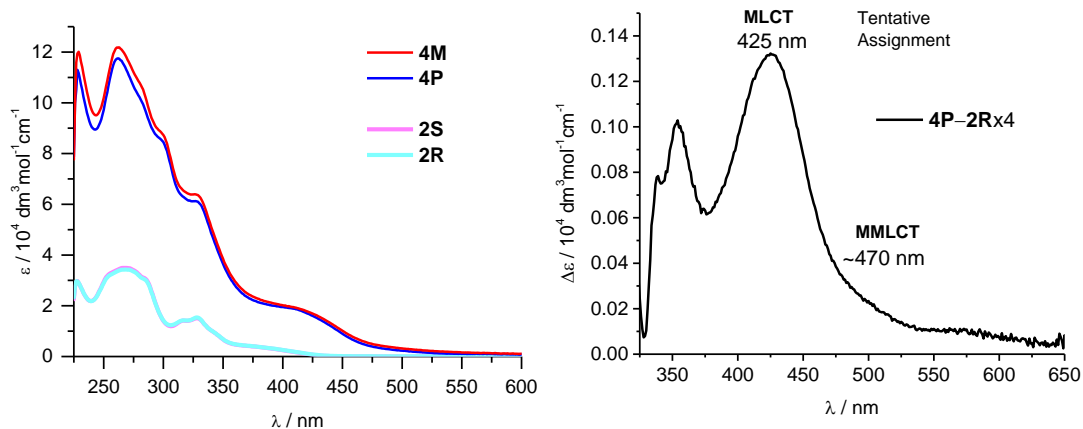


**Figure S37.** (left) UV-vis absorption spectra of **2S/2R** and **4M/4P** in  $\text{CH}_2\text{Cl}_2$  at 298 K. (right) The mathematic difference  $\Delta\varepsilon$  between **4P** and **2R** ( $\varepsilon$  values multiplied by 4).

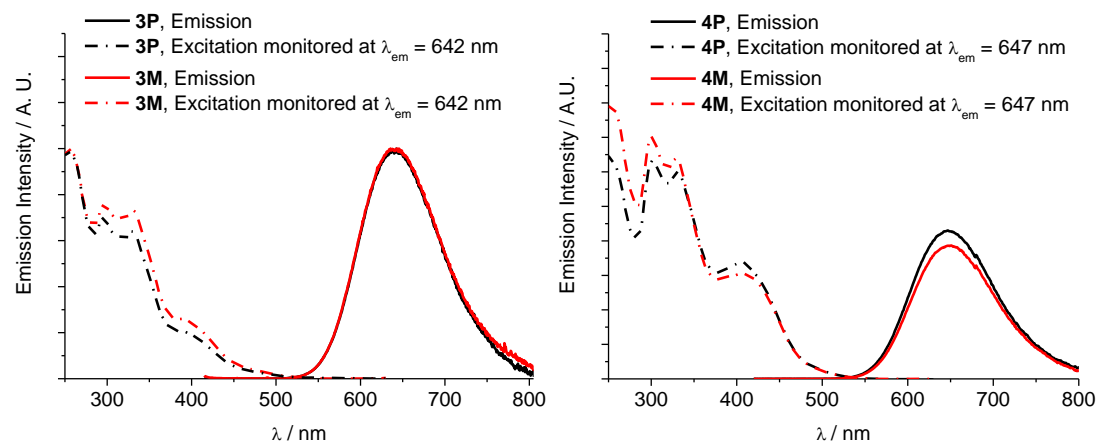


**Figure S38.** Emission and excitation spectra of (left) **3M/3P** and (right) **4M/4P** ( $1 \times 10^{-5}$  M in  $\text{CH}_2\text{Cl}_2$ ) at 298 K.

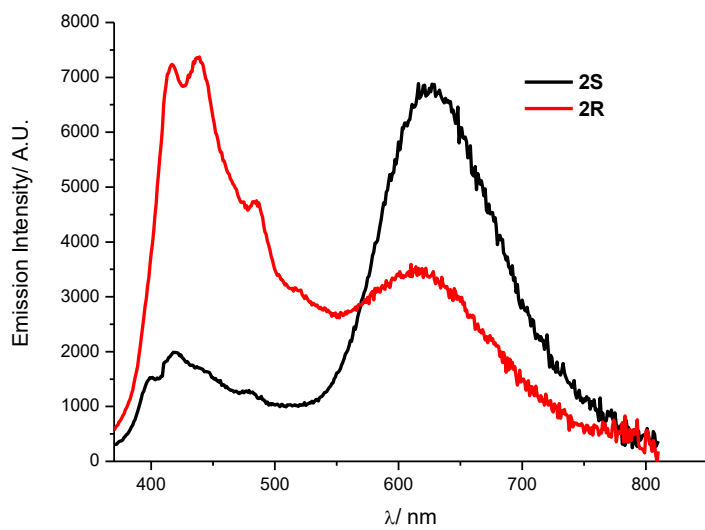


**Figure S39.** Solid emission spectra of **2S** and **2R** at 298 K ( $\lambda_{\text{ex}} = 350$  nm).

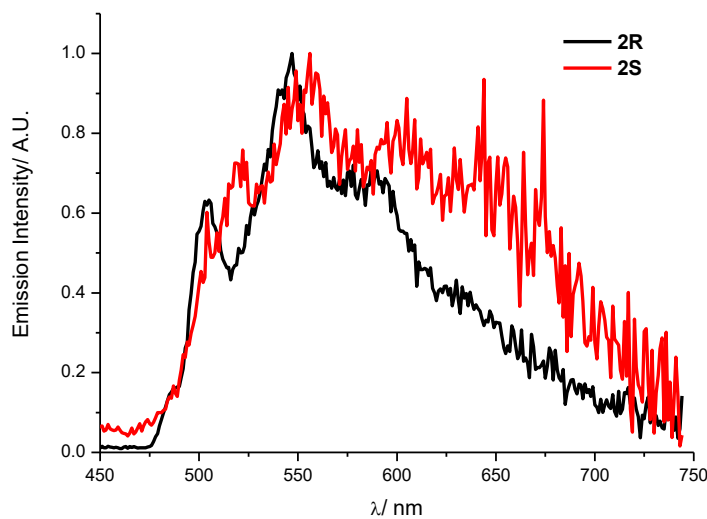


**Figure S40.** Solid emission spectra of **2S** and **2R** at 77 K ( $\lambda_{\text{ex}} = 350$  nm).

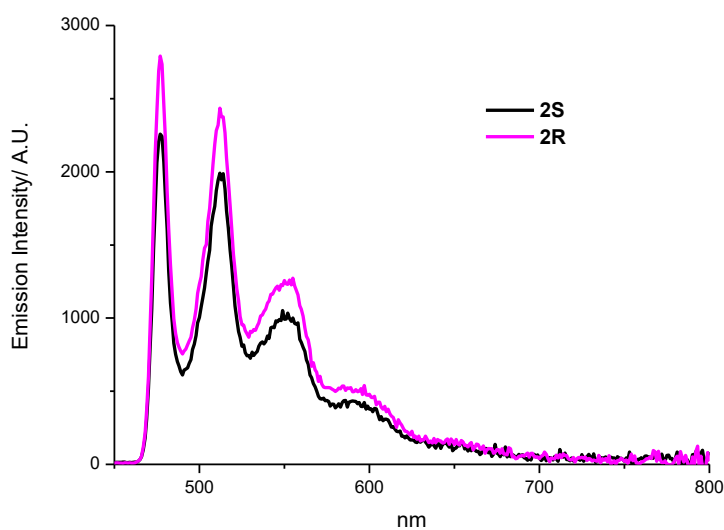


**Figure S41.** Glassy emission spectra of **2S** and **2R** ( $1 \times 10^{-5}$  M in 2-MeTHF) at 77 K ( $\lambda_{\text{ex}} = 400$  nm).

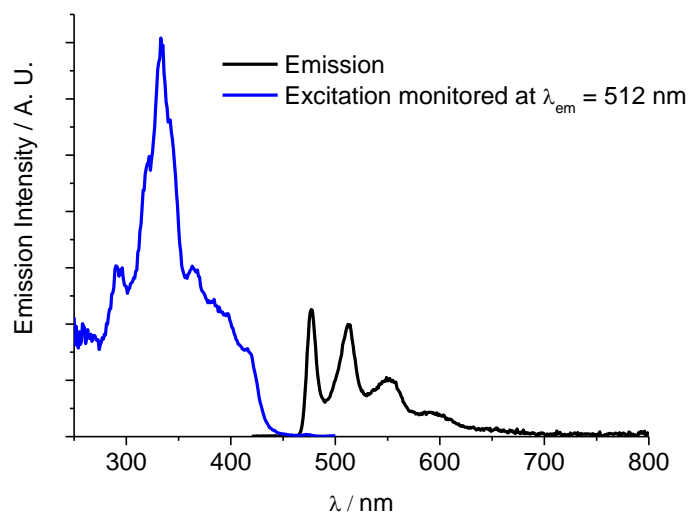


**Figure S42.** Emission and excitation spectra of **2R** ( $1 \times 10^{-5}$  M in 2-MeTHF) at 77 K.

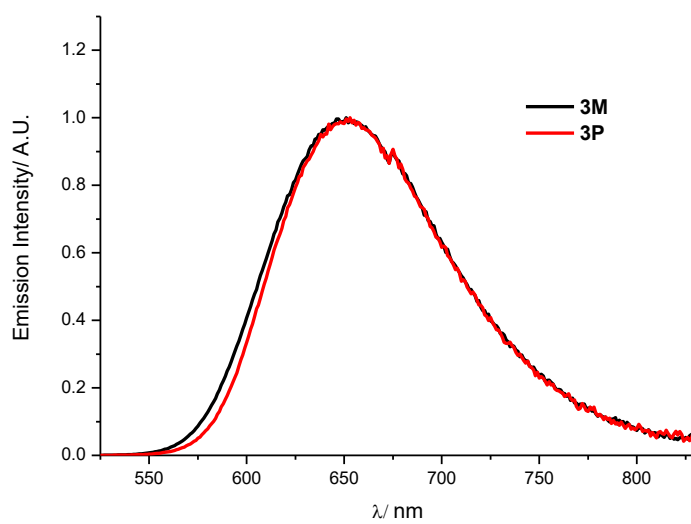


**Figure S43.** Solid emission spectra of **3M** and **3P** at 298 K ( $\lambda_{\text{ex}} = 500$  nm).

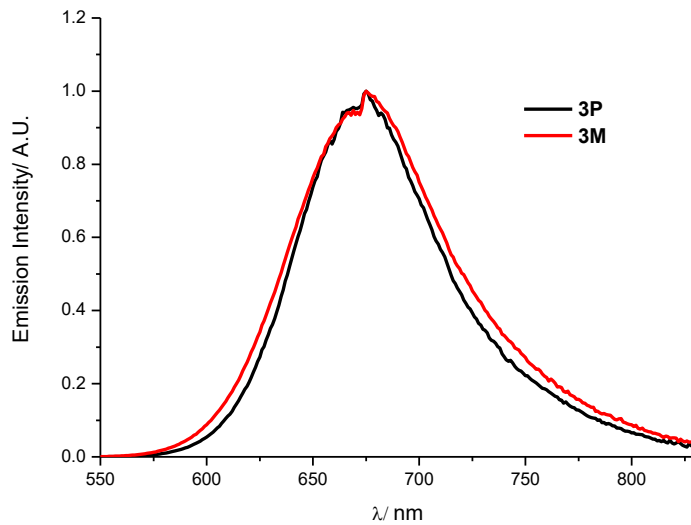


**Figure S44.** Solid emission spectra of **3M** and **3P** at 77 K ( $\lambda_{\text{ex}} = 480$  nm).

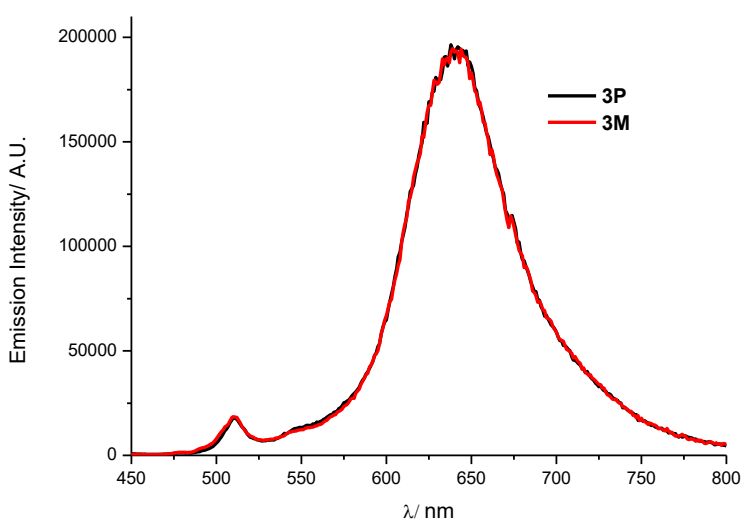


**Figure S45.** Glassy emission spectra of **3M** and **3P** ( $1 \times 10^{-5}$  M in 2-MeTHF) at 77 K ( $\lambda_{\text{ex}} = 400$  nm).

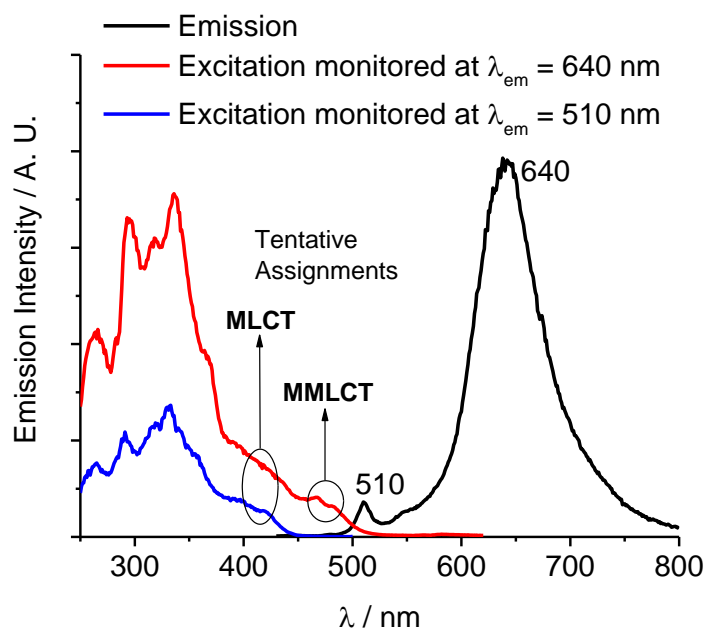


**Figure S46.** Emission and excitation spectra of **3P** ( $1 \times 10^{-5}$  M in 2-MeTHF) at 77 K.

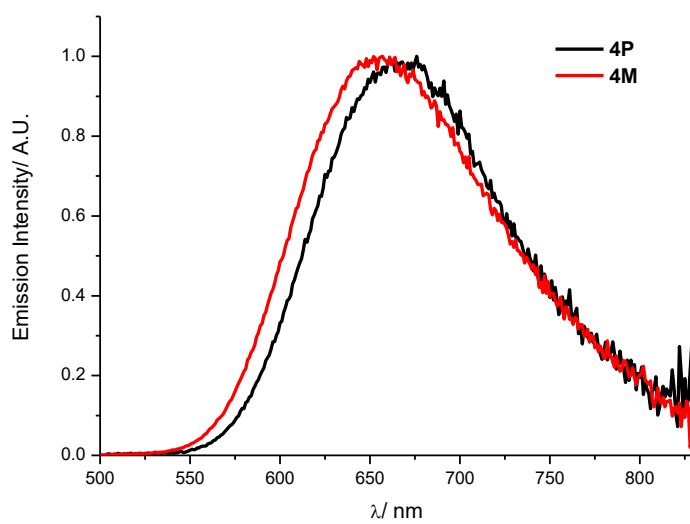


**Figure S47.** Solid emission spectra of **4M** and **4P** at 298 K ( $\lambda_{\text{ex}} = 450$  nm).

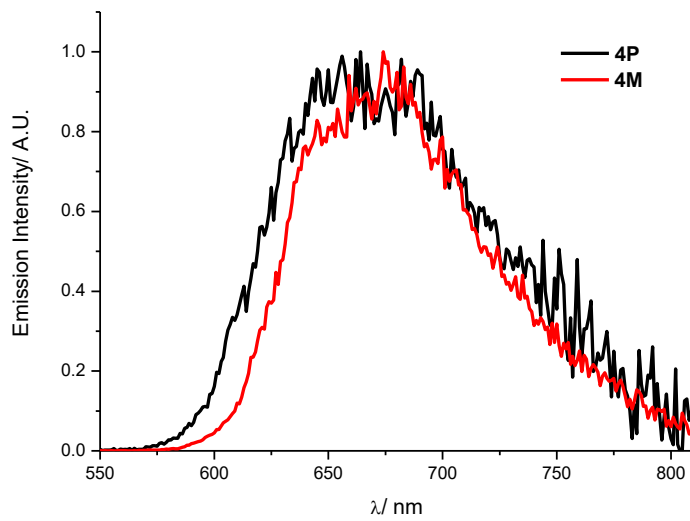


**Figure S48.** Solid emission spectra of **4M** and **4P** at 77 K ( $\lambda_{\text{ex}} = 450$  nm).

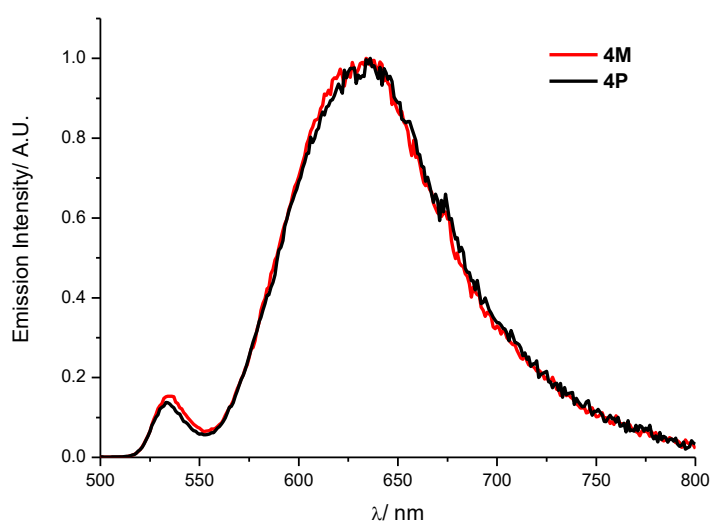


**Figure S49.** Glassy emission spectra of **4M** and **4P** ( $1 \times 10^{-5}$  M in 2-MeTHF) at 77 K ( $\lambda_{\text{ex}} = 430$  nm).

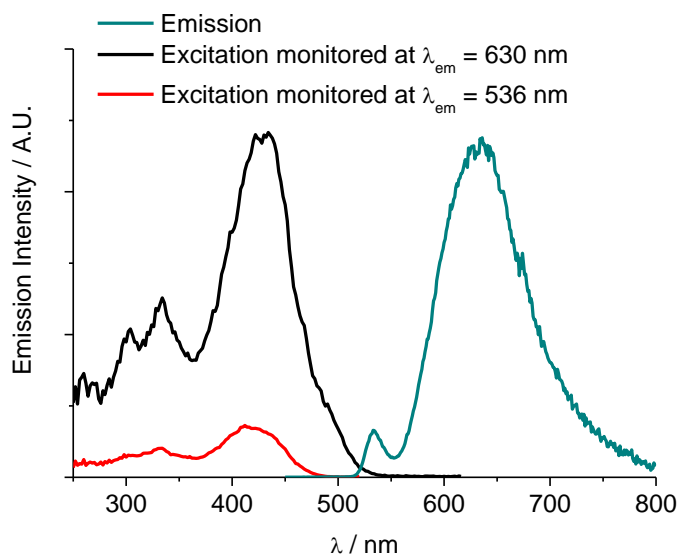


**Figure S50.** Emission and excitation spectra of **4P** ( $1 \times 10^{-5}$  M in 2-MeTHF) at 77 K.

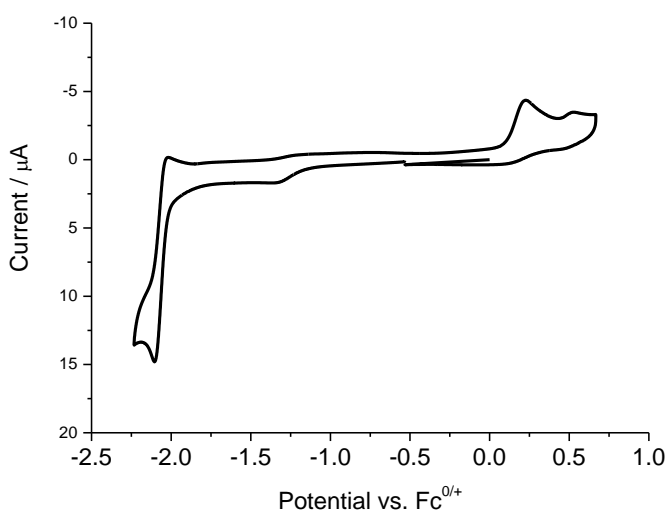


**Figure S51.** Cyclic voltammogram of **3P** in deoxygenated  $\text{CH}_2\text{Cl}_2$  solutions at 298 K (supporting electrolyte:  $0.1 \text{ mol dm}^{-3}$   ${}^n\text{Bu}_4\text{NPF}_6$ ; scan rate:  $50 \text{ mVs}^{-1}$ ).

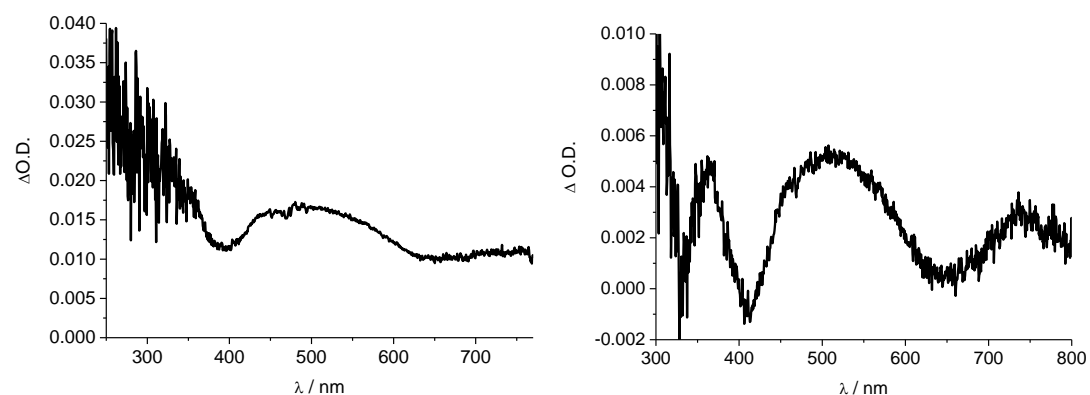


**Figure S52.** Nanosecond transient absorption spectra of (left) **3P** and (right) **4P** in a deoxygenated  $\text{CH}_2\text{Cl}_2$  solution at 298 K (concentration  $\sim 1 \times 10^{-4} \text{ mol dm}^{-3}$ ).

## Computational Results

All calculations were performed with Gaussian 09 suit of program<sup>4</sup> employing density functional theory (DFT) and time-dependent density functional theory (TDDFT). The hybrid functional B3LYP<sup>5</sup> and double zeta basis set (LanL2DZ<sup>6</sup> for Pd and 6-31G(d)<sup>7</sup> for other atoms) was applied here. The geometries of ground state folded structure were full optimized based on the X-ray crystal structures. Solvent effects were considered using the Polarizable Continuum Model (PCM)<sup>8</sup> of SCRF procedure for dichloromethane and DMSO in both optimizations and TD calculations, which was also employed experimentally. The singlet vertical excitation energy and corresponding electron transitions as well as the frontier molecular orbital analysis was based on the ground state geometry. Based on the excitation energy ( $E_{n \rightarrow m}$ ), and oscillator strengths ( $f$ ), the rotatory strength, absorption spectra and ECD spectra were simulated using Gaussian functions. According to the experimental results and the corresponding calculated absorption results, we suggest that the HOMO-1–LUMO transition which can be assigned as MMLCT will cause strong absorption and emission.

---

(<sup>4</sup>) G. W. T. M. J. Frisch, H. B. Schlegel, G. E. Scuseria, M. A. Robb, J. R. Cheeseman, G. Scalmani, V. Barone, B. Mennucci, G. A. Petersson, H. Nakatsuji, M. Caricato, X. Li, H. P. Hratchian, A. F. Izmaylov, J. Bloino, G. Zheng, J. L. Sonnenberg, M. Hada, M. Ehara, K. Toyota, R. Fukuda, J. Hasegawa, M. Ishida, T. Nakajima, Y. Honda, O. Kitao, H. Nakai, T. Vreven, J. A. Montgomery, Jr., J. E. Peralta, F. Ogliaro, M. Bearpark, J. J. Heyd, E. Brothers, K. N. Kudin, V. N. Staroverov, R. Kobayashi, J. Normand, K. Raghavachari, A. Rendell, J. C. Burant, S. S. Iyengar, J. Tomasi, M. Cossi, N. Rega, J. M. Millam, M. Klene, J. E. Knox, J. B. Cross, V. Bakken, C. Adamo, J. Jaramillo, R. Gomperts, R. E. Stratmann, O. Yazyev, A. J. Austin, R. Cammi, C. Pomelli, J. W. Ochterski, R. L. Martin, K. Morokuma, V. G. Zakrzewski, G. A. Voth, P. Salvador, J. J. Dannenberg, S. Dapprich, A. D. Daniels, Ö. Farkas, J. B. Foresman, J. V. Ortiz, J. Cioslowski, and D. J. Fox, Gaussian, Inc., Wallingford CT,, *Gaussian, Inc. Wallingford CT*, 2009.

(<sup>5</sup>) A. D. Becke, *J. Chem. Phys.*, 1993, **98**, 5648-5652.

(<sup>6</sup>) C. E. Check, T. O. Faust, J. M. Bailey, B. J. Wright, T. M. Gilbert and L. S. Sunderlin, *J. Phys. Chem. A*, 2001, **105**, 8111-8116.

(<sup>7</sup>) P. C. Hariharan and J. A. Pople, *Theor. Chim. Acta*, 1973, **28**, 213-222.

(<sup>8</sup>) V. Barone and M. Cossi, *J. Phys. Chem. A*, 1998, **102**, 1995-2001.

**Table S3.** Calculated molecular orbitals of complex **3P** in CH<sub>2</sub>Cl<sub>2</sub>.

MO	Energy / eV	Assignment
L+9	-0.005	7% dπ+dπ*, 82% pπ+pπ*
L+8	-0.233	5% dπ+dπ*, 86% pπ+pπ*
L+7	-0.292	4% dπ+dπ*, 91% pπ+pπ*
L+6	-0.86	2% dπ+dπ*, 92% pπ+pπ*
L+5	-0.919	98% pπ+pπ*
L+4	-0.988	97% pπ+pπ*
L+3	-1.29	98% pπ+pπ*
L+2	-1.478	98% pπ+pπ*
L+1	-1.772	4% dπ+dπ*, 90% pπ+pπ*
LUMO	-2.123	3% dπ+dπ*, 89% pπ+pπ*
HOMO	-5.135	27% Pd-dz <sup>2</sup> , 15% dπ+dπ*, 68% pπ+pπ*
H-1	-5.342	37% Pd-dz <sup>2</sup> , 17% Pd-dx <sup>2</sup> -y <sup>2</sup> , 50% pπ+dπ
H-2	-5.362	19% Pd-dz <sup>2</sup> , 17% Pd-dx <sup>2</sup> -y <sup>2</sup> , 61% pπ+dπ
H-3	-5.649	18% Pd-dx <sup>2</sup> -y <sup>2</sup> , 30% dπ+dπ*, 56% pπ+pπ*
H-4	-5.682	29% Pd-dx <sup>2</sup> -y <sup>2</sup> , 24% dπ+dπ*, 42% pπ+pπ*
H-5	-5.792	14% Pd-dx <sup>2</sup> -y <sup>2</sup> , 43% dπ+dπ*, 48% pπ+pπ*
H-6	-5.831	15% Pd-dx <sup>2</sup> -y <sup>2</sup> , 50% dπ+dπ*, 33% pπ+pπ*
H-7	-5.994	13% dπ+dπ*, 84% pπ+pπ*
H-8	-6.078	19% dπ+dπ*, 78% pπ+pπ*
H-9	-6.378	92% pπ+pπ*

**Table S4.** Calculated molecular orbitals of complex **3P** in DMSO.

MO	Energy / eV	Assignment
L+9	-0.386	37% d $\pi$ +d $\pi^*$ , 55% p $\pi$ +p $\pi^*$
L+8	-0.484	19% Pd-dx <sup>2</sup> -y <sup>2</sup> , 31% d $\pi$ +d $\pi^*$ , 46% p $\pi$ +p $\pi^*$
L+7	-0.563	21% d $\pi$ +d $\pi^*$ , 72% p $\pi$ +p $\pi^*$
L+6	-0.965	5% d $\pi$ +d $\pi^*$ , 92% p $\pi$ +p $\pi^*$
L+5	-0.986	5% Pd-dx <sup>2</sup> -y <sup>2</sup> , 92% p $\pi$ +p $\pi^*$
L+4	-1.33	5% Pd-dz <sup>2</sup> , 90% p $\pi$ +p $\pi^*$
L+3	-1.561	5% d $\pi$ +d $\pi^*$ , 91% p $\pi$ +p $\pi^*$
L+2	-1.671	96% p $\pi$ +p $\pi^*$
L+1	-2.085	97% p $\pi$ +p $\pi^*$
LUMO	-2.171	98% p $\pi$ +p $\pi^*$
HOMO	-5.321	13% Pd-dx <sup>2</sup> -y <sup>2</sup> , 12% d $\pi$ +d $\pi^*$ , 71% p $\pi$ +p $\pi^*$
H-1	-5.623	19% Pd-dx <sup>2</sup> -y <sup>2</sup> , 14% d $\pi$ +d $\pi^*$ , 61% p $\pi$ +p $\pi^*$
H-2	-5.908	36% Pd-dz <sup>2</sup> , 17% Pd-dx <sup>2</sup> -y <sup>2</sup> , 42% p $\pi$ +p $\pi^*$
H-3	-5.983	20% Pd-dx <sup>2</sup> -y <sup>2</sup> , 24% d $\pi$ +d $\pi^*$ , 47% p $\pi$ +p $\pi^*$
H-4	-6.016	14% Pd-dx <sup>2</sup> -y <sup>2</sup> , 23% d $\pi$ +d $\pi^*$ , 58% p $\pi$ +p $\pi^*$
H-5	-6.062	15% Pd-dz <sup>2</sup> , 25% d $\pi$ +d $\pi^*$ , 57% p $\pi$ +p $\pi^*$
H-6	-6.165	24% Pd-dz <sup>2</sup> , 37% d $\pi$ +d $\pi^*$ , 43% p $\pi$ +p $\pi^*$
H-7	-6.193	13% d $\pi$ +d $\pi^*$ , 83% p $\pi$ +p $\pi^*$
H-8	-6.47	21% Pd-dz <sup>2</sup> , 26% d $\pi$ +d $\pi^*$ , 49% p $\pi$ +p $\pi^*$
H-9	-6.547	35% Pd-dz <sup>2</sup> , 10% d $\pi$ +d $\pi^*$ , 51% p $\pi$ +p $\pi^*$

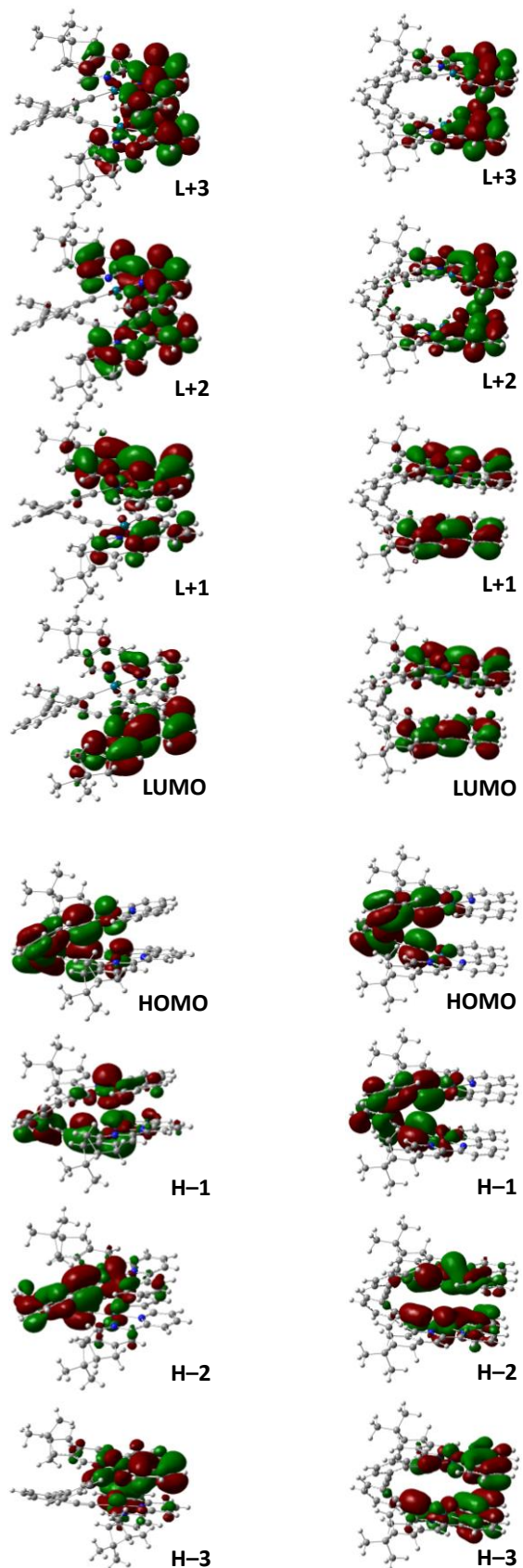


**Figure S45.** Calculated molecular orbitals of complex **3P** in  $\text{CH}_2\text{Cl}_2$  (left) and in DMSO (right).

**Table S5.** Calculated transition oscillation strength and rotatory strength of complex **3P** in CH<sub>2</sub>Cl<sub>2</sub>.

Energy / eV	Energy / nm	Oscillation Strength	Rotatory Strength	Transition Configuration
2.4013	516.32	0.0095	-8.4018	H→L 74.2%, H-1→L 21.2%
2.5908	478.55	0.0209	75.1811	H-1→L 69.5%, H→L 23.5%
2.6938	460.25	0.0176	-44.59	H-2→L 89.1%, H-1→L 7.3%
2.7349	453.34	0.008	-8.3014	H→L+1 74.3%, H-1→L+1 18.8%
2.8709	431.87	0.0044	24.3521	H-3→L 64.3%, H-4→L 31.7%
2.8982	427.8	0.0026	-16.7408	H-4→L 59.4%, H-3→L 31.8%
2.938	422	0.0106	26.4529	H-1→L+1 56.7%, H→L+1 22.7%, H-2→L+1 17.0%
3.0113	411.73	0.0199	-50.2639	H-5→L 79.7%, H-6→L 7.7%
3.0357	408.42	0.0294	-3.3924	H-2→L+1 70.8%, H-1→L+1 20.6%
3.0654	404.47	0.0067	-5.4589	H→L+2 77.9%, H-1→L+2 15.3%
3.0999	399.96	0.009	-27.1242	H-6→L 83.5%, H-5→L 7.9%
3.1987	387.6	0.005	56.6294	H-3→L+1 85.4%
3.2534	381.09	0.0242	75.3985	H-1→L+2 53.0%, H→L+3 16.7%, H→L+2 13.5%, H-1→L+3 8.4%
3.2611	380.19	0.0106	7.8522	H→L+3 53.1%, H-1→L+2 18.1%, H-1→L+3 14.4%
3.2877	377.12	0.003	17.7962	H-4→L+1 84.7%, H-3→L+1 5.6%
3.3389	371.33	0.0186	-39.7861	H-2→L+2 80.2%, H-1→L+2 5.2%
3.3684	368.08	0.063	-21.9279	H-7→L 62.7%, H-8→L 13.2%, H-6→L+1 10.1%
3.3878	365.98	0.0284	28.0655	H-6→L+1 46.8%, H-5→L+1 34.2%
3.4044	364.19	0.0068	13.3055	H-5→L+1 58.0%, H-6→L+1 25.3%
3.4582	358.52	0.0172	15.2661	H-1→L+3 47.5%, H→L+3 20.4%, H→L+4 9.2%, H-2→L+3 8.5%
3.4946	354.79	0.0196	73.803	H-8→L 53.9%, H-7→L 18.5%, H→L+4 13.5%
3.5286	351.37	0.051	-150.668	H→L+4 40.2%, H-8→L 20.5%, H-2→L+3 18.8%, H-1→L+3 10.1%
3.5436	349.89	0.0346	-68.1509	H-3→L+2 70.2%, H-9→L 6.9%, H-4→L+2 5.4%
3.5474	349.51	0.0147	5.0389	H-2→L+3 39.2%, H-4→L+2 23.7%, H→L+4 17.1%
3.5892	345.44	0.0085	21.9658	H→L+5 37.1%, H-4→L+2 32.2%, H-2→L+3 5.4%
3.6106	343.39	0.0323	37.4009	H→L+5 33.7%, H-4→L+2 22.4%, H-2→L+3 14.0%, H→L+4 7.6%, H-5→L+2 5.6%
3.65	339.68	0.0022	-3.6443	H→L+6 50.7%, H-10→L 21.1%, H-1→L+6 11.0%
3.6544	339.27	0.009	31.8582	H-10→L 25.5%, H-5→L+2 24.9%, H→L+6 18.9%, H-3→L+3 8.1%
3.696	335.45	0.0178	-6.9969	H-10→L 28.5%, H-5→L+2 25.2%, H-7→L+1 21.1%, H-8→L+1 5.3%, H-4→L+3 5.1%
3.7024	334.88	0.0549	65.1491	H-3→L+3 24.2%, H-7→L+1 20.8%, H-10→L 14.0%,

3.7202	333.27	0.0384	0.5551	H-6→L+2 30.0%, H-7→L+1 20.5%, H-3→L+3 13.4%
3.7315	332.27	0.0097	19.7001	H-1→L+4 30.9%, H-3→L+3 19.3%, H-9→L 12.4%, H-1→L+5 7.2%, H→L+5 6.0%
3.7439	331.16	0.0068	13.6678	H-6→L+2 26.9%, H-3→L+3 22.0%, H-1→L+4 20.1%, H-1→L+5 7.0%, H→L+5 5.5%
3.78	328	0.0206	-2.8078	H-2→L+4 40.0%, H-9→L 21.9%, H-4→L+3 12.9%, H-6→L+2 8.7%

**Table S6.** Calculated transition oscillation strength and rotatory strength of complex **3P** in DMSO.

Energy / eV	Energy / nm	Oscillation Strength	Rotatory Strength	Transition Configuration
2.6318	471.42682	0.0193	143.0829	H→L 97.2%
2.7382	453.10828	0.0231	-54.7265	H→L+1 96.7%
2.9173	425.29089	0.0344	-47.3934	H-1→L 89.3%
2.9976	413.89815	0.0195	20.0274	H-1→L+1 69.1%, H-2→L 20.9%
3.0637	404.96821	0.0046	84.5735	H-2→L 64.4%, H-1→L+1 20.8%
3.1205	397.59689	0.0063	-14.5591	H-3→L 34.1%, H-2→L+1 26.6%, H-4→L+1 8.9%, H-4→L 8.9%, H-3→L+1 7.0%, H-5→L 6.4%
3.1266	396.82118	0.0063	2.9606	H-4→L 32.5%, H-3→L 26.2%, H-4→L+1 13.2%, H-2→L+1 9.2%, H-3→L+1 7.6%
3.1476	394.17369	0.0069	-12.0171	H-2→L+1 36.9%, H-4→L 20.5%, H-3→L+1 17.4%
3.1782	390.37855	0.0181	-26.9567	H→L+2 88.1%
3.2705	379.36129	0.019	1.0281	H-5→L 37.4%, H-6→L 22.1%, H-5→L+1 12.4%, H-6→L+1 8.7%
3.2799	378.27406	0.0231	26.6043	H-6→L 38.1%, H-5→L 27.4%, H-5→L+1 9.0%, H-6→L+1 7.6%
3.3089	374.95878	0.0267	-19.3939	H→L+3 91.0%
3.3624	368.99271	0.0029	-1.2111	H-3→L+1 53.4%, H-4→L 23.3%, H-4→L+1 10.1%, H-3→L 9.5%
3.3888	366.11812	0.002	2.3902	H-4→L+1 61.9%, H-3→L 13.8%, H-4→L 10.8%, H-3→L+1 8.6%
3.4209	362.68266	0.048	142.7123	H→L+4 51.1%, H-5→L+1 24.5%, H-6→L 13.6%
3.4424	360.41747	0.0479	158.5829	H-5→L+1 45.1%, H→L+4 36.4%, H-6→L 5.2%
3.4436	360.29187	0.0004	0.0601	H-6→L+1 54.8%, H-5→L 15.4%, H-2→L+1 13.5%, H-8→L 5.4%
3.464	358.17006	0.0335	-36.9951	H-1→L+2 88.0%

3.5634	348.17901	0.0115	-5.1105	H-1→L+3 49.4%, H-2→L+2 31.8%, H-7→L 5.6%
3.5838	346.19708	0.0302	52.7119	H-7→L 81.7%, H-2→L+2 5.5%
3.612	343.49421	0.0052	24.629	H-2→L+2 48.5%, H-1→L+3 40.0%
3.6636	338.65627	0.0031	-6.6391	H-7→L+1 83.5%, H-1→L+4 5.3%
3.6852	336.67131	0.0014	-0.0018	H-2→L+3 60.6%, H-5→L+2 7.2%
3.7114	334.29463	0.0342	26.7535	H-8→L 58.9%, H-6→L+1 12.9%, H-9→L 6.3%, H-5→L+2 5.5%
3.7219	333.35154	0.0554	-143.6553	H-1→L+4 67.5%, H-4→L+2 6.0%, H-8→L 6.0%
3.7462	331.18923	0.0266	72.4596	H-3→L+2 70.4%
3.7731	328.82805	0.0569	-102.4251	H-8→L+1 43.3%, H-4→L+2 11.7%, H-9→L+1 7.6%, H-6→L 5.8%
3.7785	328.35811	0.0918	-96.8753	H-4→L+2 42.4%, H-8→L+1 13.7%, H-3→L+3 5.2%
3.7949	326.93908	0.0072	51.6275	H-9→L 34.4%, H-5→L+2 16.8%, H-10→L 14.8%, H-2→L+3 10.5%
3.8039	326.16554	0.0271	-25.0232	H-6→L+2 25.1%, H-10→L 19.5%, H-9→L+1 15.3%, H-9→L 10.7%, H-5→L+3 7.1%
3.8132	325.37006	0.0061	-24.201	H→L+5 77.6%, H-5→L+2 7.8%
3.8251	324.35782	0.1121	105.0183	H-5→L+2 34.9%, H-9→L 16.4%, H-8→L 10.3%, H→L+5 8.6%, H-3→L+3 7.5%
3.8378	323.28446	0.0076	12.1361	H→L+6 87.2%, H→L+5 5.9%
3.8534	321.97568	0.1384	-119.4103	H-6→L+2 24.6%, H-10→L 24.6%, H-2→L+4 14.8%, H-9→L+1 8.6%
3.8658	320.94291	0.0017	5.8854	H-3→L+3 57.7%, H-4→L+2 17.1%, H-4→L+3 5.5%, H-6→L+3 5.3%